(2)

Defense Nuclear Agency
Alexandria, VA 22310-3398

DNA-TR-89-262

The Effects on Antenna-Filtered Scintillation Parameters of Non-Zero Antenna Pointing Angles

Scott M. Frasier
Mission Research Corporation
P.O. Drawer 719
Santa Barbara, CA 93102

July 1990

Technical Report

CONTRACT No. DNA 001-87-C-0169

DESTRUCTION NOTICE:

FOR CLASSIFIED documents, follow the procedures in DoD 5200.22-M, Industrial Security Manual, Section II-19.

FOR UNCLASSIFIED, limited documents, destroy by any method that will prevent disclosure of contents or reconstruction of the document.

Retention of this document by DoD contractors is authorized in accordance with DoD 5220.22-M, Industrial Security Manual.

PLEASE NOTIFY THE DEFENSE NUCLEAR AGENCY, ATTN: CSTI, 6801 TELEGRAPH ROAD, ALEXANDRIA, VA 22310-3398, IF YOUR ADDRESS IS INCORRECT, IF YOU WISH IT DELETED FROM THE DISTRIBUTION LIST, OR IF THE ADDRESSEE IS NO LONGER EMPLOYED BY YOUR ORGANIZATION.

DISTRIBUTION LIST UPDATE

This mailer is provided to enable DNA to maintain current distribution lists for reports. We would appreciate your providing the requested information.

☐ Add the individual listed to your distribution list.

☐ Delete the cited organization/individual.

☐ Change of address.

NOTE:
Please return the mailing label from the document so that any additions, changes, corrections or deletions can be made more easily.

NAME: _____

ORGANIZATION: _____

OLD ADDRESS	CURRENT ADDRESS
_____	_____
_____	_____
_____	_____

TELEPHONE NUMBER: ( ) _____

SUBJECT AREA(s) OF INTEREST:

_____	_____
_____	_____
_____	_____

DNA OR OTHER GOVERNMENT CONTRACT NUMBER: _____

CERTIFICATION OF NEED-TO-KNOW BY GOVERNMENT SPONSOR (if other than DNA):

SPONSORING ORGANIZATION: _____

CONTRACTING OFFICER OR REPRESENTATIVE: _____

SIGNATURE: _____

CUT HERE AND RETURN

Director
Defense Nuclear Agency
ATTN TITL
Washington, DC 20305 1000

Director
Defense Nuclear Agency
ATTN: TITL
Washington, DC 20305 1000

REPORT DOCUMENTATION PAGE

Form Approved
OMB No. 0704-0188

1. AGENCY USE ONLY *(Leave blank)*	2. REPORT DATE	3. REPORT TYPE AND DATES COVERED
	900701	Technical 871001 - 881230

4. TITLE AND SUBTITLE
The Effects on Antenna-Filtered Scintillation Parameters of Non-Zero Antenna Pointing Angles

5. FUNDING NUMBERS
C - DNA-001-87-C-0169
PE - 62715H
PR - RB
TA - RB
WU - DH039580

6. AUTHOR(S)
Scott M. Frasier

7. PERFORMING ORGANIZATION NAME(S) AND ADDRESS(ES)
Mission Research Corporation
P.O. Drawer 719
Santa Barbara, CA 93102

8. PERFORMING ORGANIZATION REPORT NUMBER
MRC-R-1220

9. SPONSORING/MONITORING AGENCY NAME(S) AND ADDRESS(ES)
Defense Nuclear Agency
6801 Telegraph Road
Alexandria, VA 22310-3398

RAAE/Ullrich

10. SPONSORING/MONITORING AGENCY REPORT NUMBER
DNA-TR-89-262

11. SUPPLEMENTARY NOTES
This work was sponsored by the Defense Nuclear Agency under RDT&E RMC Code B466D RB RB 00140 RAAE 3220 A 25904D.

12a. DISTRIBUTION/AVAILABILITY STATEMENT
Approved for public release; distribution is unlimited.

12b. DISTRIBUTION CODE

13. ABSTRACT *(Maximum 200 words)*
In this report the antenna-filtered generalized power spectral density function (GPSD) for strong scintillation is derived for the general case of two different Gaussian antennas pointed in arbitrary directions relative to the transmitter-receiver line of sight. From the GPSD we obtain the normalized signal decorrelation coefficient and the filtered decorrelation distance and time. Expressions are also derived for the antenna power loss, the filtered frequency selective bandwidth, and the power impulse response function. The results are completely general with respect to pointing angle and the orientation of the antenna relative to the ionization structure. Finally, the power impulse response function is generalized to obtain the signal correlation as a function of delay at two different antennas. A method of using a complete set of correlation coefficients to generate signal realizations for a collection of antennas is outlined.

14. SUBJECT TERMS
Antenna Pointing Angles, Scintillation, GPSD, RF Propagation, Antenna-Filtering, Physics, Optics, Electromagnetics

15. NUMBER OF PAGES
50

16. PRICE CODE

17. SECURITY CLASSIFICATION OF REPORT	18. SECURITY CLASSIFICATION OF THIS PAGE	19. SECURITY CLASSIFICATION OF ABSTRACT	20. LIMITATION OF ABSTRACT
UNCLASSIFIED	UNCLASSIFIED	UNCLASSIFIED	SAR

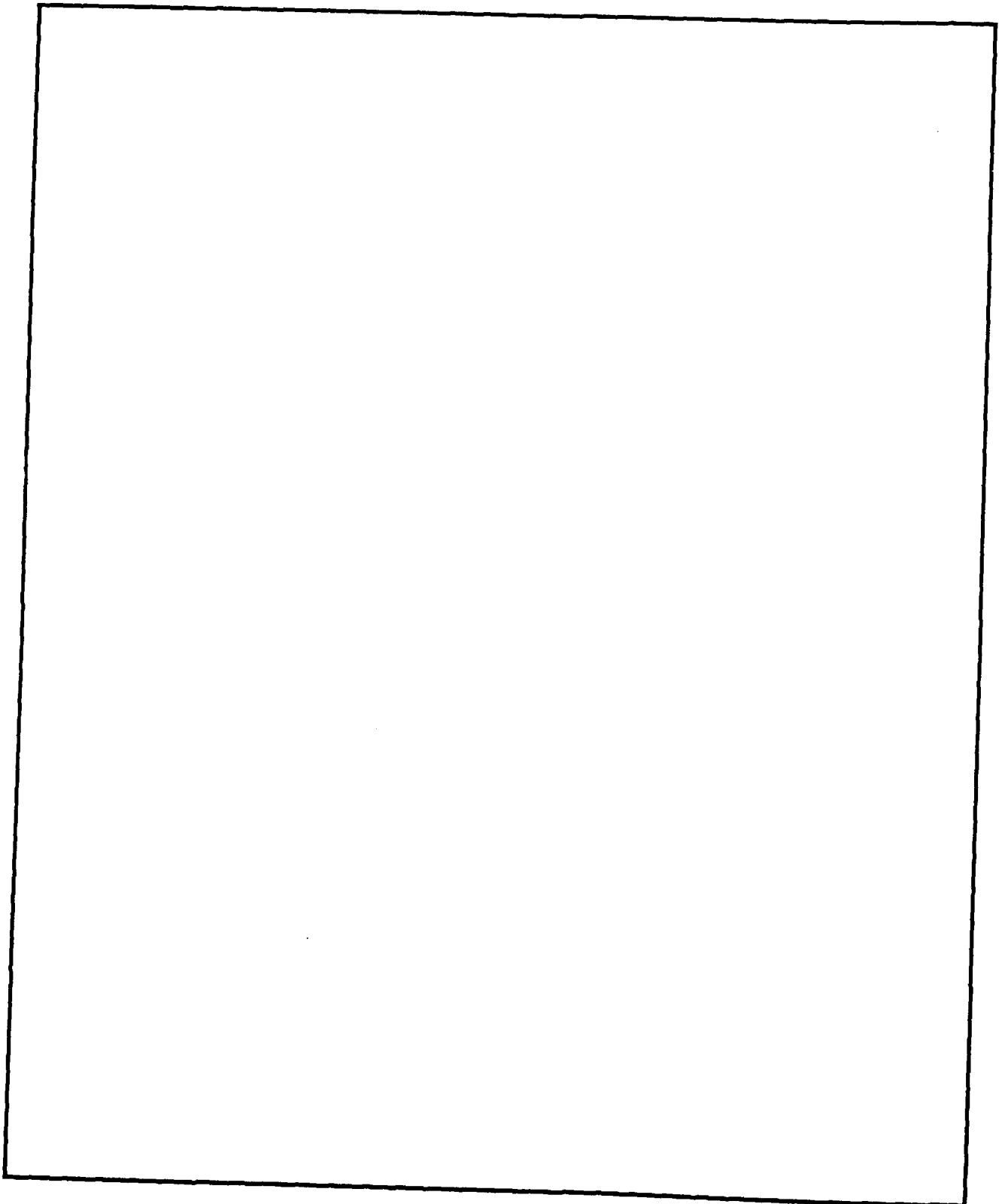

PREFACE

The author is indebted to Dr. Roger A. Dana of Mission Research Corporation with whom the author consulted often on many aspects of this research.

CONVERSION TABLE

Conversion factors for U.S. Customary to metric (SI) units of measurement

MULTIPLY →	BY →	TO GET
TO GET ←	BY ←	DIVIDE

angstrom	1.000000 x E -10	meters (m)
atmosphere (normal)	1.01325 x E +2	kilo pascal (kPa)
bar	1.000000 x E +2	kilo pascal (kPa)
barn	1.000000 x E -28	meter^2 (m^2)
British thermal unit (thermochemical)	1.054350 x E +3	joule (J)
calorie (thermochemical)	4.184000	joule (J)
cal (thermochemical) / cm^2	4.184000 x E -2	mega joule/m^2 (MJ/m^2)
curie	3.700000 x E +1	*giga becquerel (GBq)
degree (angle)	1.745329 x E -2	radian (rad)
degree Farenheit	$t_K = (t_F + 459.67)/1.8$	degree kelvin (K)
electron volt	1.60219 x E -19	joule (J)
erg	1.000000 x E -7	joule (J)
erg/second	1.000000 x E -7	watt (W)
foot	3.048000 x E -1	meter (m)
foot-pound-force	1.355818	joule (J)
gallon (U.S. liquid)	3.785412 x E -3	meter^3 (m^3)
inch	2.540000 x E -2	meter (m)
jerk	1.000000 x E +9	joule (J)
joule/kilogram (J/kg) (radiation dose absorbed)	1.000000	Gray (Gy)
kilotons	4.183	terajoules
kip (1000 lbf)	4.448222 x E +3	newton (N)
kip/inch^2 (ksi)	6.894757 x E +3	kilo pascal (kPa)
ktap	1.000000 x E +2	newton-second/m^2 (N-s/m^2)
micron	1.000000 x E -6	meter (m)
mil	2.540000 x E -5	meter (m)
mile (international)	1.609344 x E +3	meter (m)
ounce	2.834952 x E -2	kilogram (kg)
pound-force (lbs avoirdupois)	4.448222	newton (N)
pound-force inch	1.129848 x E -1	newton-meter (N·m)
pound-force/inch	1.751268 x E +2	newton/meter (N/m)
pound-force/foot^2	4.788026 x E -2	kilo pascal (kPa)
pound-force/inch^2 (psi)	6.894757	kilo pascal (kPa)
pound-mass (lbm avoirdupois)	4.535924 x E -1	kilogram (kg)
pound-mass-foot^2 (moment of inertia)	4.214011 x E -2	kilogram-meter^2 (kg·m^2)
pound-mass/foot^3	1.601846 x E +1	kilogram/meter^3 (kg/m^3)
rad (radiation dose absorbed)	1.000000 x E -2	**Gray (Gy)
roentgen	2.579760 x E -4	coulomb/kilogram (C/kg)
shake	1.000000 x E -8	second (s)
slug	1.459390 x E +1	kilogram (kg)
torr (mm Hg, 0° C)	1.333220 x E -1	kilo pascal (kPa)

*The becquerel (Bq) is the SI unit of radioactivity; 1 Bq = 1 event/s.
**The Gray (Gy) is the SI unit of absorbed radiation.

TABLE OF CONTENTS

LIST OF ILLUSTRATIONS

SECTION 1

INTRODUCTION

An electromagnetic wave that propagates through a randomly disturbed medium experiences a non-uniform phase shift across the wave front. This non-uniform phase shift causes some of the wave power to be redirected away from the propagation line-of-sight (LOS). This scattering of the wave by the random medium causes both amplitude and phase scintillation of the signal at the receiver plane. The scintillation at the receiver results from constructive and destructive interference of the contributions to the scattered field from the different parts of the wave front.

For strong scintillation, the average signal power incident on a single point in the receiver plane is the sum of the power arriving from each separate direction. However, suppose we collect the received signal over an aperture, $A_0(\vec{\rho}_0 - \vec{\rho})$, centered at $\vec{\rho}_0$ whose radius is $\sim a$. In this situation, only those scattering contributions that are of nearly uniform phase over the entire aperture will contribute significantly to the antenna-filtered output. An alternative explanation of this phenomenon can be given by considering the antenna gain function defined by

$$g_0(\vec{K}) = \int A_0(\vec{\rho}_0 - \vec{\rho}) \exp\left\{-i\vec{K} \cdot (\vec{\rho}_0 - \vec{\rho})\right\} d\vec{\rho} \tag{1.1}$$

where $\vec{K}$ is a 2-dimensional vector in the plane perpendicular to the LOS. The magnitude of $\vec{K}$ is related to the arrival angle, θ, by the formula

$$|\vec{K}| = k \sin\theta \qquad k = \frac{2\pi}{\lambda} \quad . \tag{1.2}$$

where λ is the wavelength of the carrier in free space. Plane waves arriving at an angle larger than a receiver beamwidth, $\sim \lambda/a$, with respect to the beam axis, $\hat{z}$, are rejected by the antenna; therefore, the antenna is an angle-of-arrival filter. The effects of this filtering have been investigated by Dana (1986) and Knepp (1985) for antennas pointing with their maximum gain axis along the propagation LOS. This defines the zero-pointing angle case. Dana (1986) has shown that the principal effects of antenna filtering are:

1. Power loss due to rejection by the antenna of power scattered to large angles.
2. The filtered decorrelation distance, ℓ_A, has a lower limit determined by the antenna aperture radius.
3. The filtered frequency selective bandwidth, f_A, exceeds the unfiltered value due to rejection of large-delay contributions (which arrive at large angles).

Dana also obtained the power impulse response function for the antenna-filtered signal.

In this report we extend the results of Dana (1986) to antennas that point in arbitrary directions with respect to the LOS. The principal consequence of this non-zero pointing angle is an additional power loss beyond that experienced in the zero-pointing angle case. Since the bulk of the wave power arrives along the propagation LOS, the power received by an antenna pointed at an angle of ψ_0 with respect to the LOS is reduced by a factor of approximately

$$G_0(\vec{K}(\psi_0)) = |g_0(\vec{K}(\psi_0))|^2 \quad . \tag{1.3}$$

Since scattering causes the wave power to be distributed over a spectrum of arrival angles, the exact power loss depends on the relative sizes of the signal decorrelation distance and the antenna radius, as it does in the $\psi_0 = 0$ case, as well as on the pointing angle. In this report we generally use ψ when we are referring to an antenna pointing angle measured with respect to the LOS, and we use θ to refer to an angle-of-arrival measured with respect to an axis (such as the beam axis or the LOS).

It is shown in this report that, since both the generalized power spectral density (GPSD) and the antenna gain functions are assumed to be Gaussian, the filtered decorrelation distance depends only on the antenna beamwidth and the scattering environment, but not on the pointing angle. Since the filtered decorrelation distance is the Fourier conjugate quantity to the filtered angle-of-arrival spread, $\sigma_{A\theta}$, of the received signal, and $\sigma_{A\theta}$ is not a function of the pointing angle, this result follows easily. For a non-Gaussian GPSD and/or non-Gaussian antenna gain functions, this result is only approximately true.

The filtered frequency selective bandwidth depends on both the antenna beamwidth and the antenna pointing angle. The former dependence results from the rejection of the large-delay contributions, which arrive at large angles with respect to the antenna beam axis. The pointing angle dependence results because the range of delays accepted by the antenna is proportional to the mean delay, for small ψ. The mean delay increases with increasing antenna pointing angle, so the delay spread of

the received signal increases as well. Thus, the filtered frequency selective bandwidth, being proportional to the reciprocal of the delay spread, decreases with increasing ψ. In some cases the filtered, frequency selective bandwidth, for $\psi_0 \neq 0$, can be smaller than the value obtained for a point antenna (the unfiltered value), although the power loss in these cases is usually substantial.

By a simple extention of the calculations performed for a single antenna, the filtered mutual coherence function of the signal received at two different antennas, with arbitrary pointing angles and beamwidths, is obtained. These results are used by Dana (1988) to generate properly correlated signal realizations at the outputs of a set of antennas.

In Section 2 we review the relevant scintillation results and define the antenna geometry. The unfiltered scintillation results are derived in Dana (1986) and are stated without proof in this report. The filtered GPSD is derived in Section 2 in terms of the unfiltered GPSD and the antenna gain functions $g(\vec{K})$.

In Section 3 we obtain the mean power loss for a single antenna and the filtered mutual coherence function for signals at two arbitrary antennas. From the latter, the filtered decorrelation distance and signal correlation coefficient are obtained.

In Section 4 we derive a general formula for the delay moments of the filtered GPSD. These delay moments are used to obtain the mean delay and the filtered frequency selective bandwidth, f_A. At the end of Section 4 we derive the filtered power impulse function for the received signal at a single antenna.

SECTION 2

ANTENNA-FILTERED GENERALIZED POWER SPECTRAL DENSITY

As mentioned in Section 1, antenna filtering of signals composed of a spectrum of angle-of-arrival components causes distortion of the output signal relative to the input. This distortion is not limited to a reduction in total received power; since the antenna gain for the different angular components is not uniform, scintillating signals, which contain a spectrum of angular components, experience a change in their spatial and frequency correlation characteristics when filtered by antennas. The extent of this change is dependent on the relative sizes of the angle-of-arrival spread, σ_θ, and the antenna beamwidth. If the antenna beamwidth exceeds the angle-of-arrival spread, almost all of the incident power is accepted by the antenna with a gain that is nearly independent of angle, so the antenna-filtering distortion of the signal is minimal. On the other hand, when σ_θ is larger than the antenna beamwidth, antenna filtering has the effect of reducing the effective angular spread of the signal by rejecting all components arriving at angles larger than an antenna beamwidth. Since it is the signal components arriving at the larger angles that cause the decorrelation of the signal in the receiver plane, antenna filtering generally leads to an increase in the signal decorrelation distance at the receiver plane, over its value for the unfiltered signal. In this section we derive the antenna-filtered generalized power spectral density in terms of the unfiltered GPSD and the antenna characteristics. The filtered GPSD allows us to combine the effects of the propagation environment with those of the antennas to obtain a single, antenna-filtered channel description.

Consider the antenna aperture distribution functions, $A_1(\vec{\rho}_1 - \vec{\rho})$ and $A_2(\vec{\rho}_2 - \vec{\rho})$, for two antennas centered at positions $\vec{\rho}_1$ and $\vec{\rho}_2$, respectively. The antenna profiles can be written as Fourier integrals of their respective antenna gain functions:

$$A_1(\vec{\rho}_1 - \vec{\rho}) = \frac{1}{4\pi^2} \int g_1(\vec{K}) \exp\left\{ i\vec{K} \cdot (\vec{\rho}_1 - \vec{\rho}) \right\} d\vec{K} \tag{2.1}$$

$$A_2(\vec{\rho}_2 - \vec{\rho}) = \frac{1}{4\pi^2} \int g_2(\vec{K}) \exp\left\{ i\vec{K} \cdot (\vec{\rho}_2 - \vec{\rho}) \right\} d\vec{K} \quad . \tag{2.2}$$

The gain functions, g_1 and g_2, are defined such that the antennas are aimed with zero pointing angle with respect to the line-of-sight (the $\hat{z}$ axis in this case, which

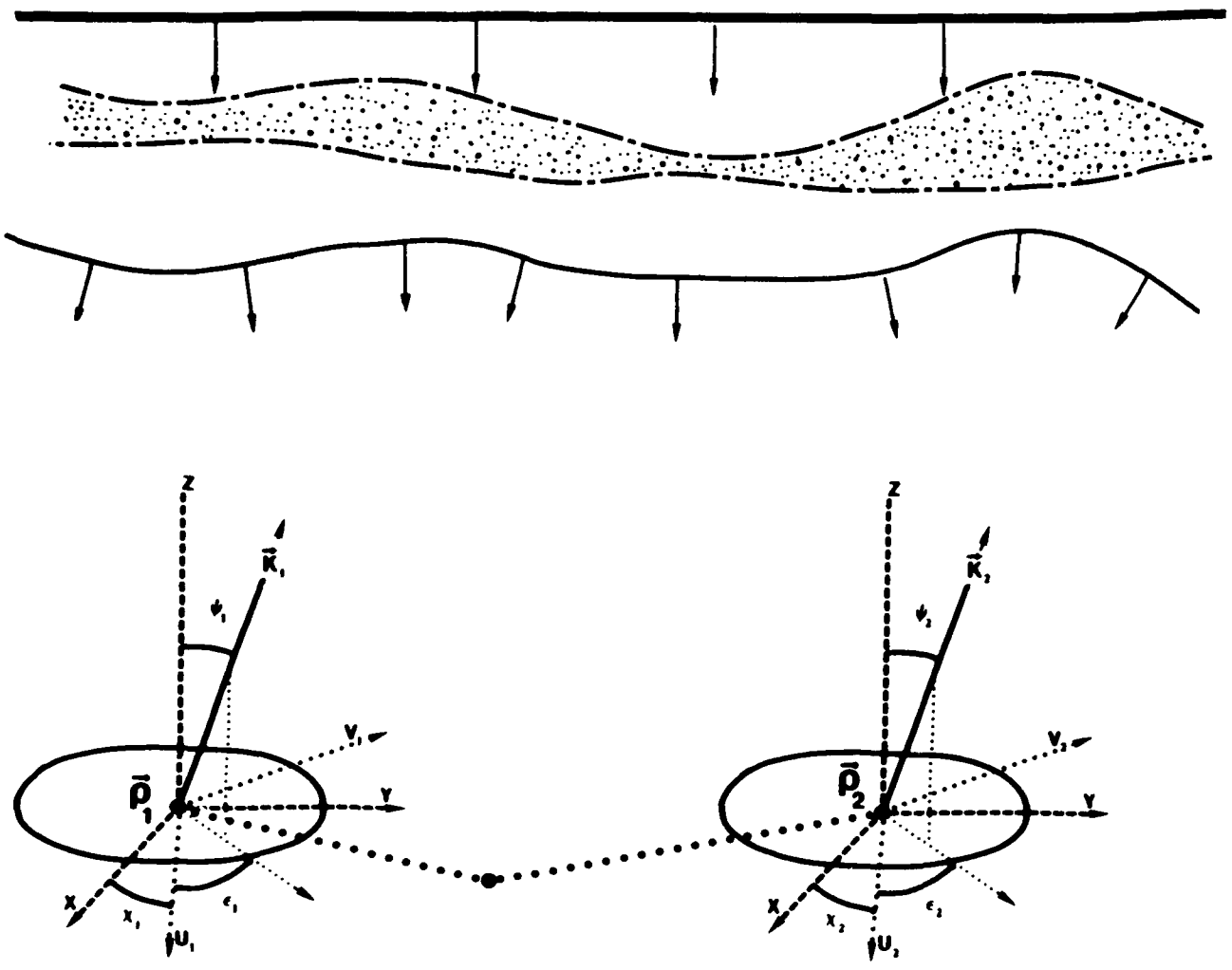

Figure 2.1. Scintillated signal incident on two arbitrary antennas.

is perpendicular to the $\vec{\rho}$-plane). See Figure 2.1. For antennas not aimed in the $\hat{z}$ direction, we must alter the antenna profiles to account for non-zero pointing angles. For small pointing angles we approximate this effect by multiplying the profile A_i by the phase factor

$$\exp\left\{i\vec{K}_i \cdot (\vec{\rho} - \vec{\rho}_i)\right\} \qquad i = 1, 2 \tag{2.3}$$

where $\vec{K}_i$ is the pointing angle vector for pointing angle ψ_i defined by

$$\vec{K}_i - \left(\vec{K}_i \cdot \hat{z}\right)\hat{z} = k \sin\psi_i \left[\cos\epsilon_i\, \hat{u}_i + \sin\epsilon_i\, \hat{v}_i\right] \tag{2.4}$$

$$|\vec{K}_i| = k \tag{2.5}$$

and k is the free space wave number for the carrier. We have defined $\vec{K}_i$ as a 3-dimensional vector in Equation 2.4 so that it more closely represents an antenna pointing direction, but the component of $\vec{K}_i$ along the LOS does not appear explicitly in any of our results. Equation 2.5 constrains the components of $\vec{K}_i$. One could define $\vec{K}_i$ as the 2-dimensional projection onto the transverse plane. In the general case, the antenna profile is not cylindrically symmetric about the beam axis so $g(\vec{K})$ depends on the orientation of the vector $\vec{K}$, not just its magnitude. For this reason, the azimuthal angle ϵ_i must be specified. (See Figure 2.1.)

The antenna-filtered complex amplitude of a signal of carrier frequency, ω_i, at time, t, is obtained by integrating the local complex amplitude, $U(\vec{\rho}', \omega_i, t)$, over the antenna aperture:

$$U_{Ai}(\vec{\rho}_i, \omega_i, t) = \int U(\vec{\rho}', \omega_i, t) A_i(\vec{\rho}_i - \vec{\rho}') \exp\left\{i\vec{K}_i \cdot (\vec{\rho}' - \vec{\rho}_i)\right\} d\vec{\rho}' \quad . \tag{2.6}$$

The mutual coherence function (MCF) for the received signal amplitudes is defined as the ensemble average of the product of the complex amplitudes of signals different frequencies, measured at different positions in the receiver plane:

$$\Gamma_A(\vec{\rho}_d, \omega_d) \equiv \langle U^*_{A2}(\vec{\rho}_2, \omega_2, t) U_{A1}(\vec{\rho}_1, \omega_1, t)\rangle \quad . \tag{2.7}$$

The statistics of the complex amplitude are assumed to be stationary in both position and frequency. Therefore, we have made use of the following defintions:

$$\vec{\rho}_d \equiv \vec{\rho}_1 - \vec{\rho}_2 \qquad \vec{\rho}_s \equiv \frac{\vec{\rho}_1 + \vec{\rho}_2}{2} \qquad \omega_d \equiv \omega_1 - \omega_2 \quad . \tag{2.8}$$

Substituting Equations 2.1, 2.2 and 2.6 into Equation 2.7, we obtain

$$\Gamma_A(\vec{\rho}_d, \omega_d) = \int \Gamma(\vec{\rho}_d', \omega_d) g_1(\vec{K}') g_2^*(\vec{K}'') \exp\left\{-i(\vec{K}' - \vec{K}_1)\cdot(\vec{\rho}' - \vec{\rho}_1)\right.$$
$$\left. + i(\vec{K}'' - \vec{K}_2)\cdot(\vec{\rho}'' - \vec{\rho}_2)\right\} \frac{d\vec{\rho}' d\vec{\rho}'' d\vec{K}' d\vec{K}''}{(2\pi)^4} \tag{2.9}$$

where $\Gamma(\vec{\rho}_d', \omega_d)$ is the unfiltered mutual coherence function analogous to Equation 2.7. Before proceeding with the evaluation of Equation 2.9, we define sum and difference variables as follows:

$$\vec{\rho}_s' \equiv \frac{\vec{\rho}'' + \vec{\rho}'}{2} \qquad \vec{\rho}_d' \equiv \vec{\rho}' - \vec{\rho}'' \tag{2.10}$$

$$\vec{K}_s' \equiv \frac{\vec{K}'' + \vec{K}'}{2} \qquad \vec{K}_d' \equiv \vec{K}' - \vec{K}'' \tag{2.11}$$

$$\vec{K}_s \equiv \frac{\vec{K}_2 + \vec{K}_1}{2} \qquad \vec{K}_d \equiv \vec{K}_1 - \vec{K}_2 \tag{2.12}$$

The coordinate transformations given above are unitary.

Substituting Equations 2.10, 2.11 and 2.12 into Equation 2.9 and performing the integrals over $\vec{\rho}_s'$ and $\vec{K}_d'$ we obtain

$$\Gamma_A(\vec{\rho}_d, \omega_d) = \int \Gamma(\vec{\rho}_d', \omega_d) g_1\left(\vec{K}_s' + \vec{K}_d/2\right) g_2^*\left(\vec{K}_s' - \vec{K}_d/2\right)$$
$$\times \exp\left\{-i(\vec{K}_s' - \vec{K}_s)\cdot(\vec{\rho}_d' - \vec{\rho}_d)\right\} \frac{d\vec{\rho}_d' d\vec{K}_s'}{4\pi^2} \quad . \tag{2.13}$$

The GPSD is defined as the Fourier transform of the MCF with respect to $\vec{\rho}_d$:

$$S(\vec{K},\omega_d) = \int \Gamma(\vec{\rho}_d,\omega_d)\, \exp\left\{-i\vec{K}\cdot\vec{\rho}_d\right\}\, d\vec{\rho}_d \quad . \tag{2.14}$$

The filtered GPSD, $S_A(\vec{K},\omega_d)$, is defined in a manner analogous to Equation 2.14, with $\Gamma(\vec{\rho}_d,\omega_d)$ replaced by $\Gamma_A(\vec{\rho}_d,\omega_d)$. The $\vec{\rho}_d'$ integral in Equation 2.13 can be completed to obtain

$$\Gamma_A(\vec{\rho}_d,\omega_d) = \int S(\vec{K}_s' - \vec{K}_s,\omega_d) g_1\left(\vec{K}_s' + \vec{K}_d/2\right) g_2^*\left(\vec{K}_s' - \vec{K}_d/2\right)$$

$$\times\, \exp\left\{i(\vec{K}_s' - \vec{K}_s)\cdot\vec{\rho}_d\right\} \frac{d\vec{K}_s'}{4\pi^2} \quad . \tag{2.15}$$

Transforming both sides of Equation 2.15 from $\vec{\rho}_d$ to its Fourier conjugate in $\vec{K}$-space, we obtain the filtered GPSD

$$S_A(\vec{K},\omega_d) = S(\vec{K},\omega_d) g_1(\vec{K}+\vec{K}_1) g_2^*(\vec{K}+\vec{K}_2) \quad . \tag{2.16}$$

The thin-layer formula for the unfiltered GPSD, $S(\vec{K},\omega_d)$, is derived in Dana (1986):

$$S(\vec{K},\omega_d) = \pi\sqrt{\|\tilde{L}\|}\, \exp\left\{-\frac{\omega_d^2\sigma_\phi^2}{2\omega^2} - \vec{K}\cdot\left[\tilde{L} + \frac{i\omega_d\Lambda\ell_0^2\omega_{coh}^{-1}\tilde{I}}{4}\right]\cdot\vec{K}\right\} \quad . \tag{2.17}$$

The anisotropy factor and coherence bandwidth are defined, respectively, as

$$\Lambda = \sqrt{\frac{2}{1+\frac{\ell_x^4}{\ell_y^4}}} \tag{2.18}$$

$$\omega_{coh} = \frac{\Lambda\omega^2 L_0^2(z_t+z_r)}{2c\sigma_\phi^2 A_2 z_t z_r} \quad . \tag{2.19}$$

In Equation 2.19 the quantity L_0 is the outer scale size of the plasma perpendicular to the magnetic field, z_t and z_r are the distances from the plasma layer to the transmitter

and receiver, respectively, and σ_ϕ^2 is the total integrated phase variance along the LOS. The constant A_2 is the coefficient of the quadratic term of the transverse autocorrelation function of the plasma electron density fluctuations. The decorrelation length matrix $\tilde{L}$ given by

$$\tilde{L} \equiv \frac{1}{4} \begin{bmatrix} \ell_x^2 & \ell_{xy}^2 \\ \ell_{xy}^2 & \ell_y^2 \end{bmatrix} \tag{2.20}$$

and ℓ_0 is the minimum decorrelation distance, which can be obtained by diagonalizing $\tilde{L}$. Dana (1986) defines the (x,y) coordinate system such that $\tilde{L}$ is diagonalized ($\ell_{xy} = 0$) and the $\hat{x}$ axis is in the direction of minimum decorrelation length ($\ell_x = \ell_0$).

The delay space analog of $S(\vec{K},\omega_d)$ is obtained by Fourier transforming $S(\vec{K},\omega_d)$ from ω_d to τ yielding

$$S(\vec{K},\tau) = \sqrt{\frac{\pi}{2}}\, \alpha \omega_{coh} \ell_x \ell_y \exp\left\{ -\frac{\alpha^2}{2} \left[\omega_{coh}\tau - \frac{\Lambda \ell_0^2 K^2}{4} \right]^2 - \vec{K} \cdot \tilde{L} \cdot \vec{K} \right\} \tag{2.21}$$

where

$$\alpha \equiv \frac{\omega}{\sigma_\phi \omega_{coh}} \tag{2.22}$$

is a dimensionless parameter that provides a measure of the relative magnitudes of the diffractive and refractive contributions to the scattering. For strong scintillation the diffractive contribution dominates and $\alpha \to \infty$. The delay space, antenna-filtered GPSD is obtained by Fourier transforming Equation 2.16:

$$\begin{aligned} S_A(\vec{K},\tau) &= \int_{-\infty}^{\infty} S_A(\vec{K},\omega_d) \exp\{i\omega_d\tau\}\, d\tau \\ &= S(\vec{K},\tau) g_1(\vec{K}+\vec{K}_1) g_2^*(\vec{K}+\vec{K}_2) \quad . \end{aligned} \tag{2.23}$$

To summarize, we have derived the GPSD and its delay space analog for the antenna-filtered signals at two different antennas at arbitrary locations and with arbitrary pointing angles. These results reduce to those of Dana (1986) when the

antennas are identical and have a pointing angle of zero. In the limit of point receivers the antenna contributions are equal to unity for all $\vec{K}$, $\vec{K}_1$ and $\vec{K}_2$, so we recover the unfiltered GPSD results from Equation 2.16 and 2.23.

The derivations presented so far in this report are not dependent on a particular form for the antenna gain function. In order to make tractable the evaluation of the filtered signal parameters, we now restrict the antenna gain functions to be Gaussian:

$$g_i(\vec{K}) = \exp\left\{-\frac{\vec{K}\cdot\tilde{\alpha}_i\cdot\vec{K}}{2}\right\} \quad . \tag{2.24}$$

The choice of Gaussian antenna gain functions implies that the antenna aperture distribution functions are also Gaussian. Although the Gaussian assumption is somewhat restrictive, the results so obtained are still approximately applicable to non-Gaussian antennas; as long as a beamwidth can be defined for the antennas considered, the antenna can be approximated by an effective Gaussian gain function. It is the size of the antenna beamwidth relative to the arrival-angle spread of the scintillating signal that largely determines the degree of antenna filtering. Deviations from the exact Gaussian form have only a small effect on the results.

Finally, in the remainder of this report it is frequently useful to explicitly evaluate result in the limit where the environment is 1-dimensional (ie. $\ell_y \gg \ell_x$). When this limit is taken the results are stated in terms of the antenna and scintillation characteristics for the x direction. The 1-dimensional antenna gain function is defined by

$$g_i(\theta_x) = \exp\left\{-\frac{(\theta_x-\psi_{0x})^2}{4\sigma_\alpha^2}\right\} \tag{2.25}$$

where θ_x is measured with respect to the antenna beam axis along the $\hat{x}$ axis and σ_α is the root mean square beamwidth. The pointing angle vector $\vec{K}_0$ is represented by the angle ψ_{0x} between the LOS and the antenna beam axis, projected onto the xz plane.

Dana (1986) defines the full-width half maximum beamwidth, θ_{0x}, such that the antenna power gain at $\theta = \theta_{0x}/2$ is 3 dB lower than its value at $\theta = 0$. It is easy to show that the antenna amplitude gain function of Equation 2.25 can be written in terms of θ_{0x} as follows:

$$g_i(\theta_x) = \exp\left\{-\frac{2\ln 2\,(\theta_x - \psi_{0x})^2}{\theta_{0x}^2}\right\} \tag{2.26}$$

$$\sigma_\alpha^2 = \frac{\theta_{0x}^2}{8\ln 2} \tag{2.27}$$

SECTION 3

FILTERED MUTUAL COHERENCE FUNCTION

In Section 2 we derived the GPSD for the antenna-filtered output of two different, arbitrarily oriented antennas. In this section we derive an explicit formula for mutual coherence function (MCF) of the received signals at two arbitrarily oriented, Gaussian antenna apertures, A_i and A_j, whose gain functions are given by Equation 2.24. The filtered MCF is obtained by Fourier transforming Equation 2.16:

$$\Gamma_A(\vec{\rho}_d, \omega_d) = \int S_A(\vec{K}, \omega_d) \, \exp\left\{ i\vec{K} \cdot \vec{\rho}_d \right\} \, \frac{d\vec{K}}{4\pi^2} \quad . \tag{3.1}$$

Equation 3.1 is easily evaluated, for the unfiltered GPSD in Equation 2.17 and Gaussian antenna gain functions. We first define the following quantities for computational convenience:

$$\tilde{Q} \equiv \tilde{L} + \frac{i\omega_d \Lambda \ell_0^2 \omega_{coh}^{-1} \tilde{I}}{4} + \frac{\tilde{\alpha}_i + \tilde{\alpha}_j}{2} \tag{3.2}$$

$$\vec{M}_{ij}(\vec{\rho}_d) \equiv \tilde{Q}^{-1/2} \cdot \vec{m}_{ij}(\vec{\rho}_d) \equiv \frac{1}{2} \tilde{Q}^{-1/2} \cdot \left[\tilde{\alpha}_i \cdot \vec{K}_i + \tilde{\alpha}_j \cdot \vec{K}_j - i\vec{\rho}_d \right] \tag{3.3}$$

$$\vec{x} \equiv \tilde{Q}^{1/2} \cdot \vec{K} + \vec{M}_{ij}(\vec{\rho}_d) \quad . \tag{3.4}$$

The result for the filtered MCF is

$$\Gamma_A(\vec{\rho}_d, \omega_d) = \sqrt{\frac{\|\tilde{L}\|}{\|\tilde{Q}\|}} \, g_2^*(\vec{K}_2) g_1(\vec{K}_1) \, \exp\left(M_{ij}^2(0) \right)$$

$$\times \, \exp\left\{ -\frac{\vec{\rho}_d \cdot \tilde{Q}^{-1} \cdot \vec{\rho}_d}{4} - i \, \vec{m}_{ij}(0) \cdot \tilde{Q}^{-1} \cdot \vec{\rho}_d \right\} \quad . \tag{3.5}$$

We note that Γ_A is a complex function of $\vec{\rho}_d$ even if the antenna profiles are real (as we choose them here), since $\tilde{Q}$ is complex and $\vec{m}_{ij}(0)$, in general, is non-zero. For $\omega_d = 0$ and $\vec{m}_{ij}(0) = 0$, Γ_A is real for all $\vec{\rho}_d$.

When we set $\omega_d = 0$ and $\vec{\rho}_d = 0$ we obtain the cross correlation of a monochromatic signal received by two arbitrary antennas located at the same position, but aimed in different directions. We expect that if the angle-of-arrival variance and the angular separation of the antennas are both comparable to or larger than the antenna beamwidths, then the two antennas accept a different set of components of the scattered radiation. Since the various components of the scattered radiation fade independently, the received signal at the two antennas should be somewhat uncorrelated. We determine the degree of decorrelation from the normalized signal correlation coefficient,

$$\begin{aligned} \rho_{12} &= \frac{\Gamma_{A12}(0)}{\sqrt{\Gamma_{A1}(0)\Gamma_{A2}(0)}} \\ &= \sqrt{\frac{\sqrt{\|\tilde{Q}_1\|\|\tilde{Q}_2\|}}{\|\tilde{Q}_{12}\|}} \exp\left\{M_{12}^2(0) - \left[\frac{M_1^2(0) + M_2^2(0)}{2}\right]\right\} \quad , \end{aligned} \tag{3.6}$$

where

$$M_i(0) \equiv M_{ii}(0) \tag{3.7}$$

$$\tilde{Q}_i \equiv \tilde{L} + \tilde{\alpha}_i \qquad \tilde{Q}_{12} \equiv \frac{\tilde{Q}_1 + \tilde{Q}_2}{2} \quad . \tag{3.8}$$

For two identical, isotropic antennas the correlation coefficient reduces to the form

$$\rho_{12} = \exp\left\{-\frac{[\vec{m}_1(0) - \vec{m}_2(0)] \cdot \tilde{Q}^{-1} \cdot [\vec{m}_1(0) - \vec{m}_2(0)]}{4}\right\} \tag{3.9}$$

where $\vec{m}_i(0) \equiv \vec{m}_{ii}(0)$. Since the two antennas receive signals that are not generally correlated, if the signal received at one antenna is fading at a particular instant it is likely that the signal at the other antenna is not, unless the depth of the fade

considered small. Thus, a two-antenna receiver scheme allows for the possibility that angular diversity can be used to mitigate the effects of deep fades.

Figure 3.1 shows the behavior of ρ_{12} for two two-antenna configurations: (1) two identical isotropic antennas both with pointing angle vectors in the xz-plane, oriented symmetrically with respect to the LOS; and (2) two identical antennas both with pointing angle vectors in the yz-plane, oriented symmetrically with respect to the LOS. The results are dependent on the ratios $\sigma_{\theta x}/\theta_0$ and $\sigma_{\theta y}/\theta_0$ and are plotted versus the scaled pointing angle, ψ_0/θ_0. Since the environment for this example is chosen to be anisotropic, the correlation behavior is different for the two configurations. Since the arrival-angle spread is larger in the x-direction than it is in the y-direction, the two antennas in configuration (1) receive a larger range of independent angular components than do the two antennas of configuration (2); therefore, the correlation coefficient for configuration (1) decreases more rapidly as a function of pointing angle than it does for configuration (2).

3.1 DECORRELATION TIME AND DISTANCES.

The decorrelation distances can be evaluated by finding the point where the magnitude of the single frequency MCF, $\Gamma_A(\vec{\rho}_d, 0)$, is reduced from its value at $\vec{\rho}_d = 0$ by e^{-1}. The term in the exponential of Equation 3.5 that is quadratic in $\vec{\rho}_d$ is solely responsible for the decorrelation with distance. Setting this term equal to one, we obtain for the decorrelation distances in the x and y directions, separately,

$$l_{Ax} = 2\sqrt{\frac{\|\tilde{Q}\|}{Q_{yy}}} \quad , \quad l_{Ay} = 2\sqrt{\frac{\|\tilde{Q}\|}{Q_{xx}}} \quad . \tag{3.10}$$

The minimum decorrelation time is obtained from the frozen-in model for motion in the direction of the smallest decorrelation distance. The antenna-filtered τ_0 is obtained by substituting $\vec{\rho}_d = \vec{V}t$ into Equation 3.5 and solving for the time for which Γ_A is reduced by e^{-1}. This yields

$$\tau_A = \sqrt{\frac{4}{\vec{V} \cdot \tilde{Q}^{-1} \cdot \vec{V}}} \quad . \tag{3.11}$$

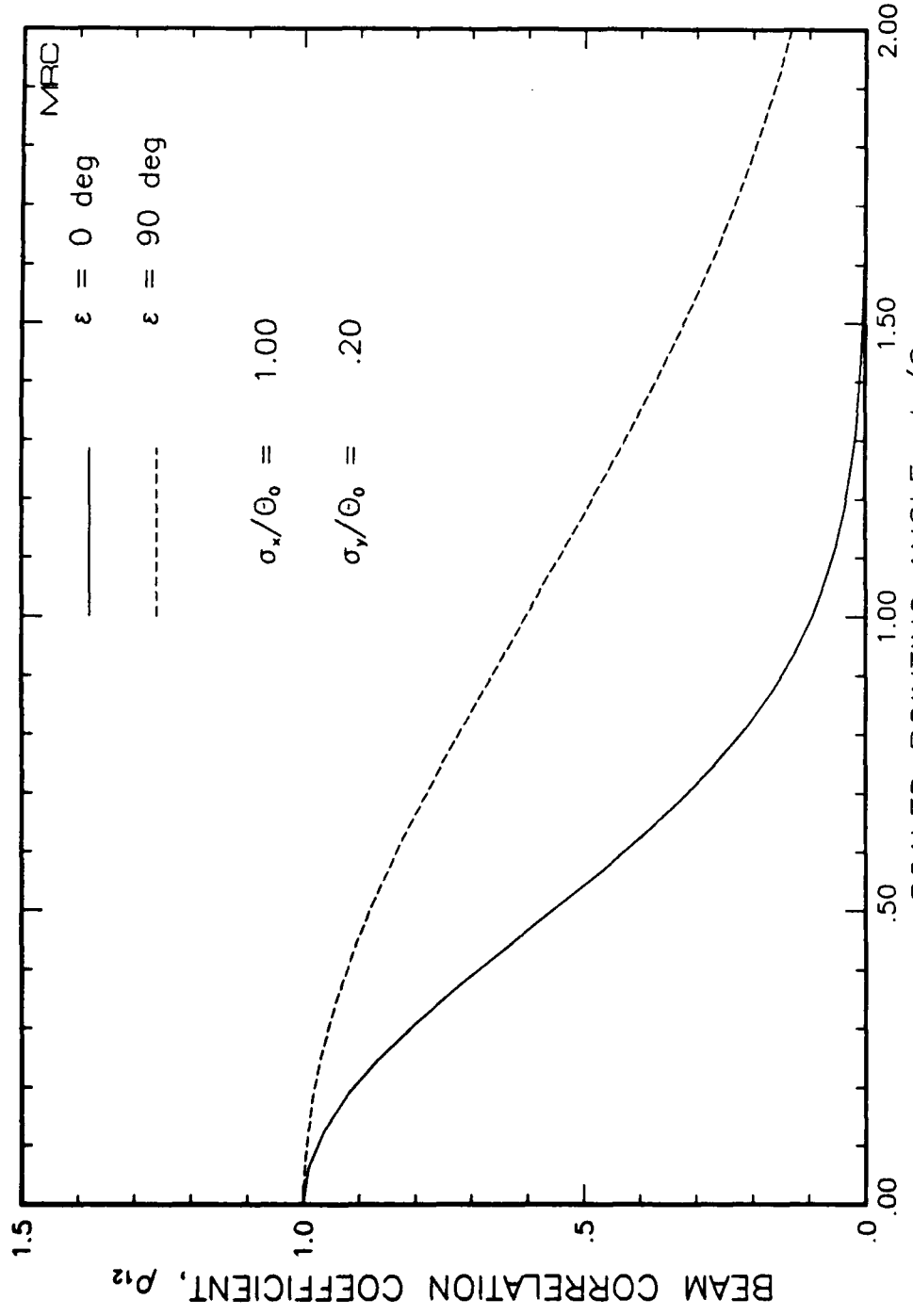

Figure 3.1. Filtered signal correlation vs. pointing angle.

If we assume that the minimum filtered decorrelation distance, ℓ_A, occurs in the x direction, and that the unfiltered τ_0 has also been obtained using the frozen-in model, we express the filtered minimum decorrelation time in the form

$$\tau_A = \frac{2\tau_0}{\ell_0}\sqrt{\frac{\|\tilde{Q}\|}{Q_{vv}}} \quad . \tag{3.12}$$

Since the scintillation environment is usually much more anisotropic than are the antenna profiles, we expect that the direction of minimum filtered decorrelation distance should be nearly the same as in the unfiltered case. The exact direction of minimum decorrelation is found by diagonalizing $\tilde{Q}$ and choosing the direction associated with the smallest eigenvalue. Notice that the decorrelation time and distances are independent of the pointing angles. The normalization of the correlation function is dependent on the pointing angles but, evidently, the functional form is not.

While the total absence of a pointing angle dependence in the decorrelation distances and time results from the Gaussian approximations used for both the antenna gain functions and the GPSD, this pointing angle independence is still present to lowest order when non-Gaussian functions are used. The decorrelation distances and time depend on the angular spread of the received signal at the antenna. The standard deviation of the angle-of-arrival is not strongly affected by the pointing angle (for a narrow beam antenna it largely controlled by the antenna beamwidth); therefore, since the decorrelation distance is the Fourier conjugate of the angle-of-arrival spread, it should not depend strongly on the pointing angle. In other words, while the exact pointing angle independence of the decorrelation distances and decorrelation time is an artifact resulting from the Gaussian approximations used, as long as we can define a meaningful antenna beamwidth and angle-of-arrival variance the result is still approximately true.

SECTION 4

DELAY MOMENTS AND THE POWER IMPULSE RESPONSE FUNCTION

If we restrict our attention to a single antenna, the correlation coefficient of Equation 3.6 is equal to unity, since it has been evaluated for a single frequency. For a modulated signal, which is a mixture of different frequencies, the different frequency components are dispersed both by propagation through a dispersive medium (that is, where the refractive index is a function of frequency), and because different frequencies are scattered to different degrees by a random medium, even if it is non-dispersive. It is this diffraction, resulting from scintillation, that dominates for strongly scintillating environments. The effect of dispersion is to distort the time profile of a transmitted wave form, since the different frequency components arrive at the receiver with different time delays; if all frequencies arrive with the same delay, the signal is not distorted, it is merely delayed. (Strictly speaking, a monochromatic wave is not delayed, since it is of infinite extent in time; however, the definition of group velocity applies to arbitrarily narrow frequency intervals.) A convenient device for investigating the scintillation distortion is the the power impulse response function,

$$G_A(\tau) = \int S_A(\vec{K},\tau)\,\frac{d\vec{K}}{4\pi^2} \tag{4.1}$$

which is the time profile function for the ensemble-averaged, antenna-filtered, received signal power resulting from the transmission of a signal impulse, $\delta(t)$. The transmitted signal impulse leaves the transmitter with an infinitesimal time spread; however, it arrives at the receiver, not only with a mean delay, $\langle\tau\rangle$, but with a delay spread, σ_τ. The delay spread depends primarily on the dispersive properties of the signal scintillation channel; when the scintillation is not strong the dispersive properties of the medium have a small influence on the delay spread.

In this section we evaluate the delay moments, $\langle\tau^n\rangle$, of the power impulse response function. The $n = 0$ moment is just the total power,

$$P_A = \int_{-\infty}^{\infty} G_A(\tau)\,d\tau \quad , \tag{4.2}$$

received by the antenna; the n^{th} moment is given by

$$\langle \tau^n \rangle = P_A^{-1} \int_{-\infty}^{\infty} \tau^n \, G_A(\tau) \, d\tau \quad ; \tag{4.3}$$

and the delay variance is given by

$$\sigma_\tau^2 = \left\langle \tau^2 \right\rangle - \langle \tau \rangle^2 \quad . \tag{4.4}$$

Although we derive the power impulse response function later in this section, it is convenient to evaluate the delay moments directly from the filtered GPSD, $S_A(\vec{K}, \tau)$, rather than from G_A. Before proceeding, we recall that the delay moments can also be derived from

$$S_A(\omega_d) = \int S_A(\vec{K}, \omega_d) \, \frac{d\vec{K}}{4\pi^2} \tag{4.5}$$

which can be regarded as a generating function for the delay moments. The mean delay and delay variance can be obtained by differentiating $S_A(\omega_d)$ with respect to ω_d and setting $\omega_d = 0$. It is easy to show that

$$\langle \tau \rangle = - \left\{ \frac{i}{S_A(\omega_d)} \, \frac{\partial S_A(\omega_d)}{\partial \omega_d} \right\}_{\omega_d = 0} \tag{4.6}$$

$$\sigma_\tau^2 = - \left\{ \frac{\partial}{\partial \omega_d} \left(\frac{1}{S_A(\omega_d)} \, \frac{\partial S_A(\omega_d)}{\partial \omega_d} \right) \right\}_{\omega_d = 0} \quad . \tag{4.7}$$

However, in this report we evaluate the delay moments of $G_A(\tau)$ using Equations 4.1 and 4.3 rather than from Equations 4.6 and 4.7.

The τ^n moments are obtained by integrating the filtered GPSD over all $\vec{K}$ and τ to obtain the average power arriving at a receiver (if both antennas are identical and they point in the same direction; otherwise the result represents the one-position two-antenna correlation)

$$P_A \langle \tau^n \rangle = \int \tau^n \, G_0(\vec{K}) S(\vec{K}, \tau) \, \frac{d\tau \, d\vec{K}}{4\pi^2} \quad . \tag{4.8}$$

where we have used Equation 2.21. The single-antenna power gain function given by

$$G_0(\vec{K}) \equiv |g_0(\vec{K})|^2 = \exp\left\{-\vec{K}\cdot\tilde{\alpha}_0\cdot\vec{K}\right\} \quad . \tag{4.9}$$

Equation 4.8 is evaluated by using the following variable changes, some of which are analogous to those defined in Equations 3.2 through 3.4:

$$\xi \equiv \alpha\left[\omega_{coh}\tau - \frac{\Lambda\ell_0^2K^2}{4}\right] \tag{4.10}$$

$$\tilde{Q} \equiv \tilde{L} + \tilde{\alpha}_0 \tag{4.11}$$

$$\vec{M} \equiv \tilde{Q}^{-1/2}\cdot\vec{m} \equiv \tilde{Q}^{-1/2}\cdot\tilde{\alpha}_0\cdot\vec{K}_0 \quad . \tag{4.12}$$

The average received power is given by Equation 4.8 with $n = 0$ obtaining

$$P_A = \sqrt{\frac{\|\tilde{L}\|}{\|\tilde{Q}\|}}\, G_0(\vec{K}_0)\, \exp\left\{\vec{m}\cdot\tilde{Q}^{-1}\cdot\vec{m}\right\} \quad . \tag{4.13}$$

The 1-dimensional limit, $\ell_y \gg \ell_x$, of Equation 4.13 is given by

$$P_A = \frac{1}{\sqrt{1+\dfrac{\sigma_{\theta x}^2}{\sigma_\alpha^2}}}\, \exp\left\{-\frac{\psi_{0x}^2}{2(\sigma_\alpha^2+\sigma_{\theta x}^2)}\right\} \tag{4.14}$$

$$\sigma_{\theta x}^2 = \frac{2}{k^2\ell_x^2} \quad . \tag{4.15}$$

Figure 4.1 shows the relative power gain of an antenna as a function of the scaled pointing angle (ψ_0/θ_0). Again the relevant parameters that determine the results are the ratios σ_x/θ_0 and $\sigma_y\theta_0$. The solid curve represents the relative power gain for an antenna whose pointing angle vector is oriented in the xz-plane and the dashed line represents the corresponding quantity for antenna oriented in the yz-plane. Since power is more widely scattered in the x direction than in the y direction the relative power gain is less sensitive to pointing angle variations in the xz-plane than in the yz-plane. The approximately 4 dB loss for $\psi_0 = 0$ results from antenna filtering; the

additional loss occurring at non-zero angles results primarily because the antenna axis is not oriented along the direction of maximum signal power (the LOS).

The higher moments of τ are evaluated by substituting the variable changes of Equations 4.10 through 4.12 into Equation 4.8, and performing the $d\xi$ integral. After some manipulation and using the expression for P_A given in Equation 4.13, we obtain

$$\langle \tau^n \rangle = \frac{4\sqrt{\pi}}{(\alpha\omega_{coh})^n} \sum_{j=0}^{j\leq n/2} 2^j \begin{pmatrix} n \\ 2j \end{pmatrix} \Gamma(j+1/2) \left(\frac{\Lambda\alpha\ell_0^2}{4}\right)^{n-2j} T_{n-j}(\vec{m},\tilde{Q}) \qquad (4.16)$$

where $\begin{pmatrix} n \\ 2j \end{pmatrix}$ is the binomial coefficient, Γ is the gamma function, and

$$T_m(\vec{m},\tilde{Q}) \equiv \frac{1}{4\pi^2} \int \left[(\vec{x}-\vec{M})\cdot\tilde{Q}^{-1}\cdot(\vec{x}-\vec{M})\right]^m \exp(-x^2)\, d\vec{x} \qquad (4.17)$$

$$\vec{x} \equiv \tilde{Q}^{-1/2}\cdot\vec{K} + \vec{M} \quad . \qquad (4.18)$$

In the strong scintillation limit ($\alpha \to \infty$), Equation 4.16 reduces to

$$\langle \tau^n \rangle = 4\pi \left(\frac{\Lambda\ell_0^2}{4\omega_{coh}}\right)^2 T_n(\vec{m},\tilde{Q}) \quad . \qquad (4.19)$$

4.1 MEAN DELAY.

Setting $n = 1$ in Equation 4.16 or Equation 4.19 we obtain the mean delay

$$\langle \tau \rangle = \frac{\pi\Lambda\ell_0^2}{\omega_{coh}} T_1(\vec{m},\tilde{Q}) \quad . \qquad (4.20)$$

Equation 4.17 evaluated for $m = 1$ reduces to

$$T_1(\vec{m},\tilde{Q}) = \frac{1}{4\pi}\left[\vec{m}\cdot\tilde{Q}^{-2}\cdot\vec{m} + \frac{\mathrm{tr}\,\tilde{Q}}{2\|\tilde{Q}\|}\right] \quad . \qquad (4.21)$$

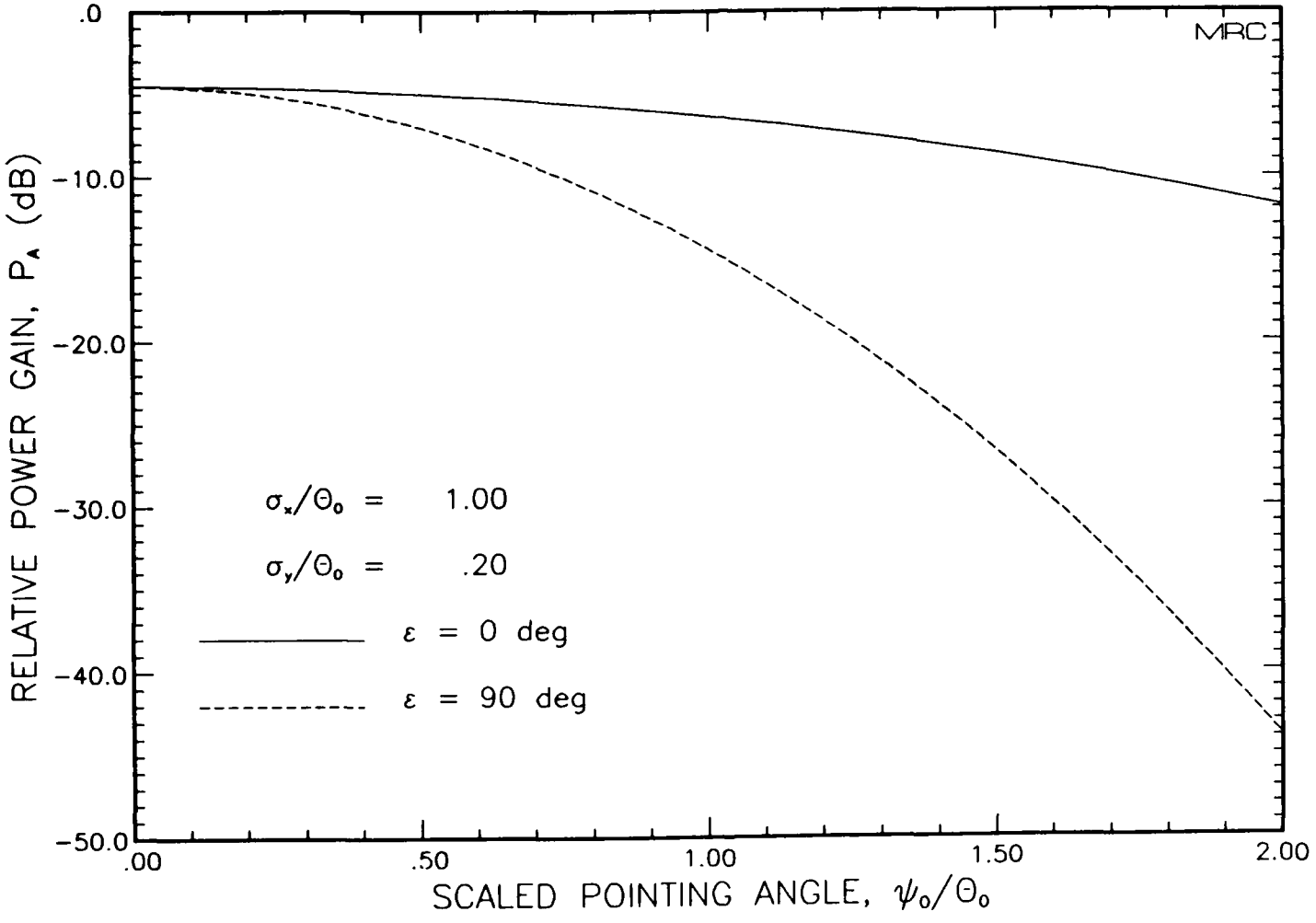

Figure 4.1. Relative power gain vs pointing angle.

The final result for the mean delay is

$$\langle \tau \rangle = \frac{\Lambda \ell_0^2}{4\omega_{coh}} \left[\vec{m} \cdot \tilde{Q}^{-2} \cdot \vec{m} + \frac{\mathrm{tr}\, \tilde{Q}}{2\|\tilde{Q}\|} \right] \quad . \tag{4.22}$$

The mean delay increases as the pointing angle increases; it is a minimum for $\psi_0 = 0$. Equation 4.22 agrees with the result of Dana (1986) for the $\psi = 0$ case.

4.2 FREQUENCY SELECTIVE BANDWIDTH.

To obtain the filtered frequency selective bandwidth for the received voltage with antenna effects we first evaluate the variance of the delay, σ_τ^2. Then, since the frequency selective bandwidth is the Fourier conjugate of the delay spread we define the filtered frequency selective bandwidth as

$$f_A \equiv \frac{1}{2\pi\sigma_\tau} \quad . \tag{4.23}$$

The second moment of $S_A(\vec{K}, \tau)$ is calculated from Equation 4.16

$$\left\langle \tau^2 \right\rangle = \frac{4\pi}{(\alpha\omega_{coh})^2} \left[T_0 + \left(\frac{\Lambda \alpha \ell_0^2}{4} \right)^2 T_2 \right] \tag{4.24}$$

and T_0 and T_2 are given by

$$T_0(\vec{m}, \tilde{Q}) = \frac{1}{4\pi} \tag{4.25}$$

and

$$T_2(\vec{m}, \tilde{Q}) = \frac{1}{4\pi} \left\{ \left(\vec{m} \cdot \tilde{Q}^{-2} \cdot \vec{m} \right)^2 + \frac{\mathrm{tr}\, \tilde{Q} \left(\vec{m} \cdot \tilde{Q}^{-2} \cdot \vec{m} \right)}{\|\tilde{Q}\|} \right.$$

$$\left. + 2\, \vec{m} \cdot \tilde{Q}^{-3} \cdot \vec{m} + \frac{3}{4} \left(\frac{\mathrm{tr}\, \tilde{Q}}{\|\tilde{Q}\|} \right)^2 - \frac{1}{\|\tilde{Q}\|} \right\} \quad . \tag{4.26}$$

Substituting the expressions for T_0 and T_2 into Equation 4.24, and substituting it and Equation 4.22 into Equation 4.4, we have for the delay variance

$$\sigma_\tau^2 = \frac{1}{(\alpha\omega_{coh})^2} + \frac{\Lambda^2\ell_0^4}{8\omega_{coh}^2}\left[\vec{m}\cdot\tilde{Q}^{-3}\cdot\vec{m} + \frac{\mathrm{tr}\,\tilde{Q}^2}{4\|\tilde{Q}\|^2}\right] \quad . \tag{4.27}$$

The filtered frequency selective bandwidth for $\alpha \to \infty$ is

$$f_A = \frac{f_0\sqrt{\mathrm{tr}\,\tilde{L}^2}}{\|\tilde{L}\|\sqrt{4\vec{m}\cdot\tilde{Q}^{-3}\cdot\vec{m} + \dfrac{\mathrm{tr}\,\tilde{Q}^2}{\|\tilde{Q}\|^2}}} \tag{4.28}$$

and the 1-dimensional limit is

$$f_A = \frac{f_0\left(1+\dfrac{\sigma_\theta^2}{\sigma_\alpha^2}\right)}{\sqrt{1+\dfrac{2\sigma_\theta^2\psi_{0x}^2}{\sigma_\alpha^2\left(\sigma_\alpha^2+\sigma_\theta^2\right)}}} \tag{4.29}$$

where $f_0 = \omega_{coh}/2\pi$. The form of the result is chosen to emphasize its invariance with respect to coordinate system choices. The frequency selective bandwidth reduces to f_0 when the antenna is omnidirectional ($\tilde{\alpha}_0$ approaches zero). For a particular antenna profile and environment ($\tilde{\alpha}_0$ and $\tilde{L}$) the maximum f_A occurs when the pointing angles are zero ($\vec{m} = 0$).

Figure 4.2 shows the antenna-filtered frequency selective bandwidth as a function of scaled pointing angle (ψ_0/θ_0). For this example, $\sigma_{\theta x} = \theta_0$; therefore, substantial antenna filtering is present in the x direction. Antenna filtering restricts the range of delays present in the received signal if the pointing angle is zero. This causes the antenna-filtered frequency selective bandwidth to be larger than the unfiltered value. As the antenna pointing angle increases the range of delays corresponding to the antenna beamwidth also increases. The larger range of delays in the received signal corresponds to a smaller antenna-filtered frequency selective bandwidth. The solid line in Figure 4.2 represents results for pointing angles in the xz plane. For the large pointing angles the value of f_A is actually smaller than the unfiltered value. The dashed curve represents results for pointing angles in the yz plane. Since $\sigma_{\theta y} = .2\theta_0$

there is less antenna filtering of f_0 resulting from the y direction. Therefore, the antenna filtering is less sensitive to pointing angle changes in the y direction than it is for the x direction. The relative power gain at a given pointing angle is also considerably smaller for the y direction than it is for the x direction.

The above formulas require the calculation of $\tilde{Q}^n$ for various values of n. Since $\tilde{Q}$ is a 2×2 matrix, it is easy to show that an arbitrary integral power of $\tilde{Q}$ can be written as a linear combination of the identity matrix $\tilde{I}$ and $\tilde{Q}$ itself,

$$\tilde{Q}^n = q_I(n)\tilde{I} + q_Q(n)\tilde{Q} \quad , \tag{4.30}$$

where the coefficients, $q_I(n)$ and $q_Q(n)$, are functions of n, tr $\tilde{Q}$, and $\|\tilde{Q}\|$. This property facilitates the efficient evaluation of quantities such as $\vec{m} \cdot \tilde{Q}^{-3} \cdot \vec{m}$. The coefficients, $q_I(n)$ and $q_Q(n)$, can be evaluated successively by multiplying the characteristic equation for $\tilde{Q}$,

$$\tilde{Q}^2 - \left(\text{tr}\,\tilde{Q}\right)\tilde{Q} + \|\tilde{Q}\|\,\tilde{I} = 0 \quad , \tag{4.31}$$

by powers of $\tilde{Q}$. The forward and backward recursion relations for $q_I(n)$ and $q_Q(n)$ can be shown to be

$$\begin{aligned} q_Q(n+1) &= \text{tr}\,\tilde{Q}\, q_Q(n) + q_I(n) & \qquad q_I(n+1) &= -\|\tilde{Q}\|\, q_Q(n) \\ q_Q(n-1) &= -\frac{q_I(n)}{\|\tilde{Q}\|} & \qquad q_I(n-1) &= q_Q(n) + \frac{\text{tr}\,\tilde{Q}}{\|\tilde{Q}\|}\, q_I(n) \end{aligned} \tag{4.32}$$

with the boundary conditions $q_I(0) = 1$ and $q_Q(0) = 0$.

4.3 POWER IMPULSE RESPONSE FUNCTION.

For the infinitesimal delay interval $\delta\tau$, $G_A(\tau)\,\delta\tau$, represents the ensemble average of the received power in the delay interval centered at τ, when the transmitted signal is the impulse function, $\delta(t)$. We evaluate G_A in the limit where $\alpha \to \infty$. In this limit we have

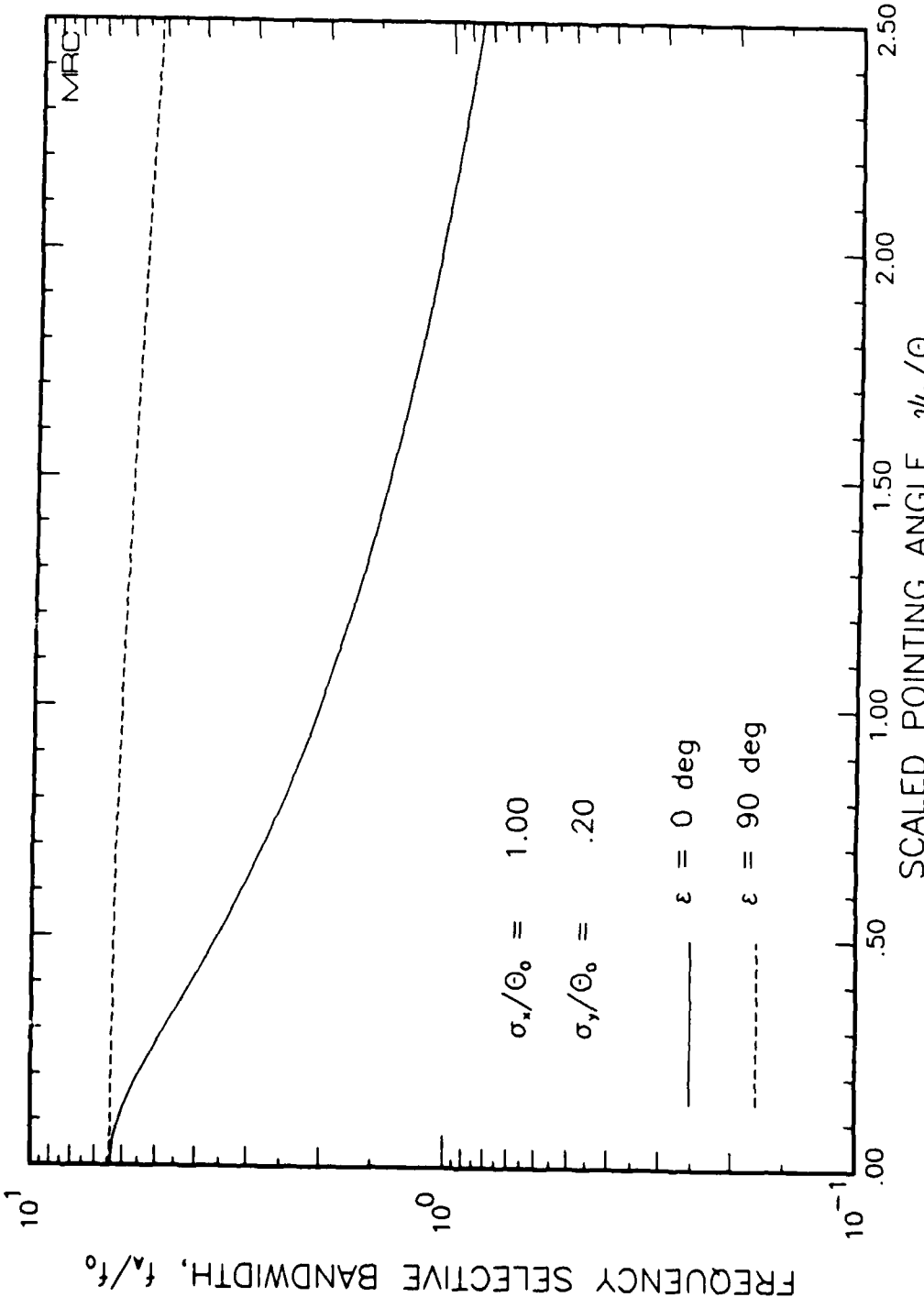

Figure 4.2. Antenna-filtered frequency selective bandwidth vs pointing angle.

$$\lim_{\alpha\to\infty} S(\vec{K},\tau) = \frac{4\pi\omega_{coh}\ell_y}{\Lambda\ell_x}\,\exp\left\{-\vec{K}\cdot\tilde{L}\cdot\vec{K}\right\}\,\delta\left(K^2-\frac{4\omega_{coh}\tau}{\Lambda\ell_0^2}\right) \tag{4.33}$$

$$\lim_{\alpha\to\infty} S_A(\vec{K},\tau) = G_0(\vec{K}+\vec{K}_0)\lim_{\alpha\to\infty} S(\vec{K},\tau) \tag{4.34}$$

where we have used Equations 2.23 for the single antenna case, $g_2(\vec{K}_2) = g_1(\vec{K}_1)$.

Evaluating the integral over $d|\vec{K}|$ in Equation 4.1 with Equation 4.34, we reduce the power impulse response function to a one-dimensional integral over the cylindrical polar angle, ϕ,

$$G_A(\tau) = \frac{\omega_{coh}\ell_y G_0(\vec{K}_0)}{2\pi\Lambda\ell_x}\int_0^{2\pi}\exp\left[-a(\tau)+b(\tau)\cos 2\phi + c(\tau)\cos(\phi-\phi_0)\right]\,d\phi \quad . \tag{4.35}$$

Equation 4.35 includes the following definitions:

$$a(\tau) = \frac{2\omega_{coh}\tau}{\Lambda\ell_0^2}\,\mathrm{tr}\,\tilde{Q} \tag{4.36}$$

$$b(\tau) = \frac{2\omega_{coh}\tau}{\Lambda\ell_0^2}\sqrt{(\,\mathrm{tr}\,\tilde{Q})^2 - 4\|\tilde{Q}\|} \tag{4.37}$$

$$c(\tau) = 4\sqrt{\frac{\omega_{coh}\tau}{\Lambda\ell_0^2}}\,|\tilde{\alpha}\cdot\vec{K}_0| \tag{4.38}$$

$$\phi_0 = \phi_\alpha - \phi_Q + \frac{\pi}{2} \tag{4.39}$$

$$\tan\phi_\alpha = \frac{\alpha_u^2\cos\epsilon\sin\chi + \alpha_v^2\sin\epsilon\cos\chi}{\alpha_u^2\cos\epsilon\cos\chi - \alpha_v^2\sin\epsilon\sin\chi} \tag{4.40}$$

$$\tan 2\phi_Q = \frac{2Q_{xy}}{Q_{xx}-Q_{yy}} \quad . \tag{4.41}$$

We evaluate the angular integral in Equation 4.35 by making use of the series expansion (formula 9.6.34, Abramowitz and Stegun 1965)

$$\exp(z\,\cos\theta) = I_0(z) + 2\sum_{\mathsf{k}=1}^{\infty} I_{\mathsf{k}}(z)\,\cos\,\mathsf{k}\theta \tag{4.42}$$

twice. The resulting double series is evaluated term by term to yield the single series

$$G_A(\tau) = \frac{\omega_{coh}\ell_y G_0(\vec{K}_0)}{\Lambda\ell_z}\,\exp\{-a(\tau)\}\left[I_0(b(\tau))I_0(c(\tau)) + 2\sum_{\mathsf{k}=1}^{\infty} I_{\mathsf{k}}(b(\tau))I_{2\mathsf{k}}(c(\tau))\cos\,2\mathsf{k}\phi_0\right] \quad . \tag{4.43}$$

Figure 4.3 gives the power impulse reponse function as a function of delay for antennas with pointing angles of zero and $\theta_0/2$. The solid line corresponds to an antenna with a pointing angle of zero, the dashed line corresponds to one pointed at an angle of $\theta_0/2$ in the xz-plane ($\epsilon = 0$ deg), and the dotted line corresponds to one pointed at an angle of $\theta_0/2$ in the yz-plane ($\epsilon = 90$ deg). All of the results have been scaled by the total mean power gain, $G_0(\psi_0)$. Since θ_0 is larger than σ_y the primary effect of non-zero pointing angles is on the mean power gain; on the other hand, since σ_z is comparable to θ_0 the relative filtering of the arrival angle components, and hence the delay components, is dependent on the pointing angle. Figure 4.3 illustrates this phenomenon.

In the limit where the pointing angle approaches zero, $c(\tau) \rightarrow 0$ and Equation 4.43 reduces to the result of Dana (1986)

$$G_A(\tau)|_{\vec{K}_0=0} = \frac{\omega_{coh}\ell_y}{\Lambda\ell_z}\,\exp\{-a(\tau)\}\;I_0(b(\tau)) \quad . \tag{4.44}$$

When $b(\tau)$ and $c(\tau)$ are not too large, the result in Equation 4.43 can be evaluated efficiently using backward recursion to generate the modified Bessel functions. For other cases it is necessary to evaluate the integral in Equation 4.35 numerically.

The 1-dimensional limit of Equation 4.43 is obtained by first noting that $b(\tau) \rightarrow \infty$ as $\ell_y/\ell_z \rightarrow \infty$. The factors of $I_{\mathsf{k}}(b(\tau))$ have the asymptotic limiting form

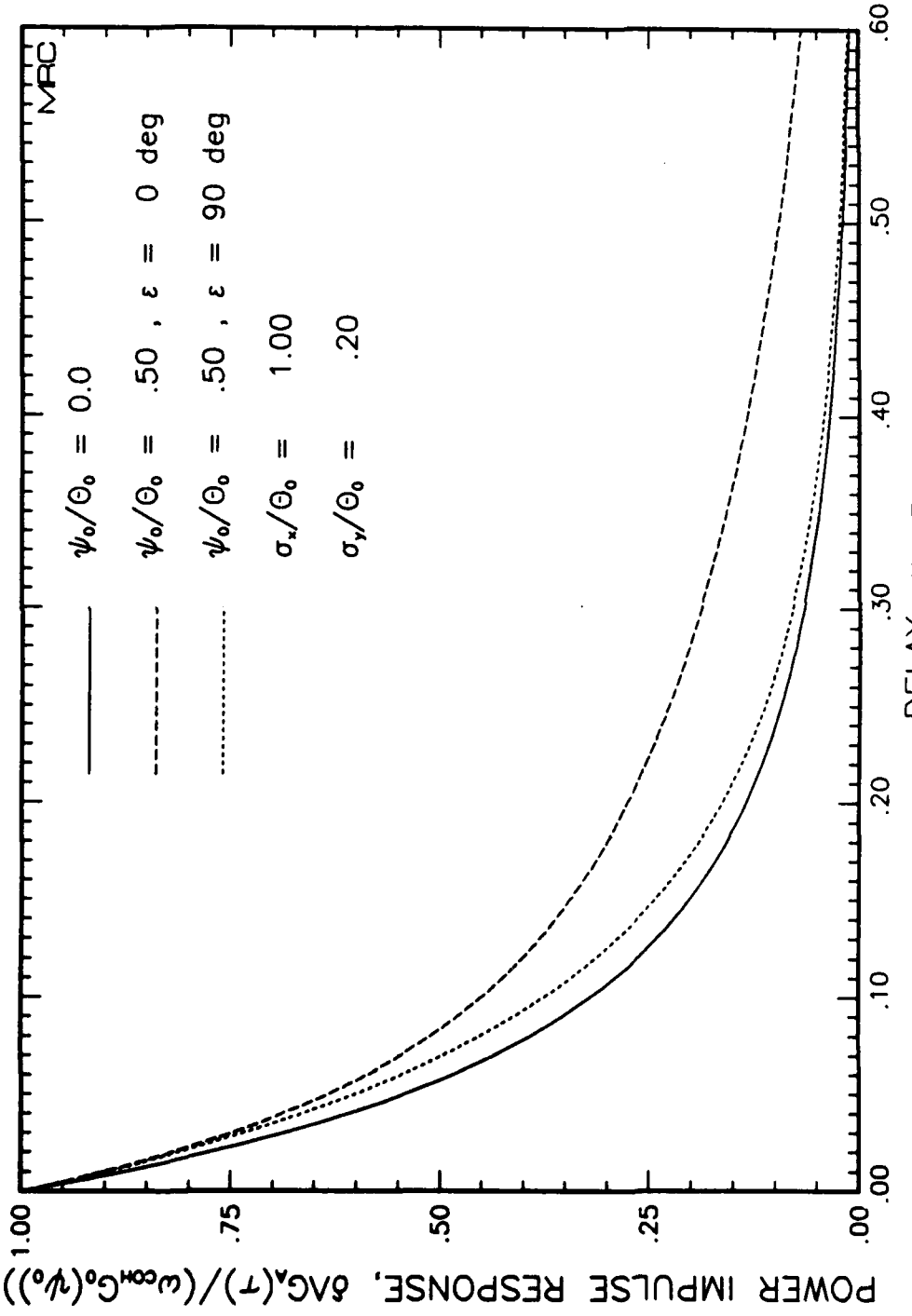

Figure 4.3. Power impulse response function vs delay.

$$I_k(b(\tau)) \sim \frac{1}{\sqrt{2\pi b(\tau)}} \exp\{b(\tau)\} \qquad b(\tau) \gg \mathbf{k} \quad . \tag{4.45}$$

Since the asymptotic form of the I_k is independent of k, we remove the common factor from each term of the series in Equation 4.43 and apply Equation 4.42 to the remaining series and obtain the asymptotic formula

$$\begin{aligned} G_A(\tau) &= \lim_{\ell_y \gg \ell_z} \frac{\omega_{coh}\ell_y G_0(\theta_0)}{\Lambda \ell_z \sqrt{2\pi b(\tau)}} \exp\{-a(\tau)+b(\tau)\} \cosh\left(c(\tau)\cos\phi_0\right) \\ &= \sqrt{\frac{\sqrt{2}\, f_0}{\tau}} \exp\left\{-\sqrt{2}\pi f_0 \tau \left(1+\frac{\sigma_\theta^2}{\sigma_\alpha^2}\right) - \frac{\psi_{0x}^2}{2\sigma_\alpha^2}\right\} \cosh\left(\sqrt{8\pi f_0 \tau}\, \frac{\sigma_\theta \psi_{0x}}{\sigma_\alpha^2}\right) \quad . \end{aligned} \tag{4.46}$$

4.4 IMPULSE RESPONSE CORRELATION.

So far in this section the function $G_A(\tau)$ has been evaluated for a single antenna. We now generalize this function for two antennas. Consider the function

$$G_{Aij}(\tau) = \exp\left\{i\vec{K}_s \cdot \vec{\rho}_d + i\vec{K}_d \cdot \vec{\rho}_s\right\} \int S_A(\vec{K},\tau) \exp\left\{i\vec{K}\cdot\vec{\rho}_d\right\} \frac{d\vec{K}}{4\pi^2} \tag{4.47}$$

which represents the impulse response correlation function of the received field at two antennas, located $\vec{\rho}_d$ apart. The correlation is a function of delay. The integral over all τ is equal to $\Gamma_A(\vec{\rho}_{ij}, \omega_d = 0)$. Since the received signals are delta-correlated in delay, properly correlated realizations of signals received at a set of N_A antennas are generated merely by maintaining the correct impulse response correlations at each delay, separately. At each simulation time, t, and for each time delay, $\mathbf{k}\Delta\tau$, we represent the received signal set as a vector

$$\vec{h}_A(t,\mathbf{k}) = \tilde{H}^A(\mathbf{k}) \cdot \vec{Z}(t,\mathbf{k}) \tag{4.48}$$

where $\vec{h}^A = (h_{A1}, \ldots, h_{AN_A})$, $\tilde{H}^A$ is the impulse response generation matrix, and $\vec{Z} = (Z_1, \ldots, Z_{N_A})$ is a set of independent Gaussian random variable sequences. The impulse response generation matrix is chosen such that the condition

$$\tilde{G}_A(\mathbf{k}) = \{G_{Aij}(\mathbf{k})\} = \tilde{H}^{A\dagger}(\mathbf{k}) \cdot \tilde{H}^A(\mathbf{k}) \tag{4.49}$$

is satisfied. Both the $\tilde{G}_A$ and $\tilde{H}^A$ are Hermitian matrices. The procedure for obtaining $\tilde{H}^A$ from $\tilde{G}_A$ is as follows:

1. Solve the eigenvalue equation

$$\|\tilde{G}_A(\mathbf{k}) - \gamma(\mathbf{k})\tilde{I}\| = 0 \tag{4.50}$$

   for both the eigenvalues $\gamma_i(\mathbf{k})$ and the corresponding eigenvectors $\hat{e}_i(\mathbf{k})$.

2. Obtain the orthonormal transformation

$$\tilde{O}(\mathbf{k}) = \left[\left[\hat{e}_1 \right] \left[\hat{e}_2 \right] \ldots \left[\hat{e}_{\mathbf{k}} \right] \right] \quad . \tag{4.51}$$

3. Obtain the real diagonal matrix $\tilde{G}_A^D(\mathbf{k})$ with the similarity transformation

$$\tilde{G}_A^D(\mathbf{k}) = \tilde{O}^\dagger(\mathbf{k}) \cdot \tilde{G}_A(\mathbf{k}) \cdot \tilde{O}(\mathbf{k}) \quad . \tag{4.52}$$

4. The diagonal impulse response generation matrix is defined as

$$\tilde{H}^A(\mathbf{k}) = \sqrt{\tilde{G}_A^D(\mathbf{k})} \quad . \tag{4.53}$$

5. The impulse response generation is obtained by the inverse similarity transformation

$$\tilde{H}^A(\mathbf{k}) = \tilde{O}(\mathbf{k}) \cdot \tilde{H}_D^A(\mathbf{k}) \cdot \tilde{O}^\dagger(\mathbf{k}) \quad . \tag{4.54}$$

We showed in Section 3 that the filtered decorrelation time is independent of pointing angle, so if all of the antennas are isotropic and have the same beamwidth, it is possible to characterize the signal decorrelation time for the set of antennas by a single number, τ_A. This property allows the generation of the correlated signals from a set of independent Rayleigh signal generators all of which have the same decorrelation time; the size of the set of signal generator is $N_A \times N_D$ where N_D is the number of delay samples. The impulse response generation matrices all have dimension $N_A \times N_A$.

SECTION 5

SUMMARY

In this report we have extended the antenna filtering results derived by Dana (1986) to include cases where the antennas are pointed at non-zero angles with respect to the LOS. We have also introduced the concepts of angular diversity and impulse response correlation of signals received at a set of antennas.

In addition to reducing total received power, non-zero pointing angles also alter the frequency and delay space character of the filtering. The principal reason for this alteration is that a non-zero pointing angle causes the antenna to receive a different mixture of angular components than that obtained for a pointing angle of zero. Generally speaking, the larger the pointing angle the larger the mean delay and delay spread and the smaller the antenna-filtered frequency selective bandwidth.

Since antennas located at the same position but with different pointing angles have different filtering characteristics, it is possible to receive more than one signal at the same position by using different antennas. If the antennas are pointed in sufficiently different directions, the fading characteristics of the received signals from the set of antennas are somewhat decorrelated. This decorrelation provides allows for the possibility of obtaining a diversity gain since there is a reduced likelyhood that all of the antennas in the set experience a deep fade simultaneously. The price to be paid for this angular diversity is a reduction in the net gain of each antenna in the set. The reduced gain limits the magnitude of the diversity gain obtainable.

Finally, we have discussed the concept of impulse response correlation. By generalizing the definition of the power impulse response function to a set of antennas we have derived the correlation of the received signal at a set of antennas as a function of delay. Using these delay dependent correlation matrices we have outlined a method for generating properly correlated signals at a set of receiver from a set of independent Rayleigh signals, in the special case in which the filtered decorrelation times at all of the antennas are equal. This method may be useful for efficiently generating continuous, properly correlated, antenna-filtered Rayleigh signals for arbitrary time durations.

SECTION 5

LIST OF REFERENCES

1. Abramowitz, Milton and Irene A. Stegun, *Handbook of Mathematical Functions*, New York: Dover Publications, Inc., 1965.

2. Dana, R. A., *Propagation of RF Signals Through Structured Ionization: Theory and Antenna Aperture Effect Applications*, DNA-TR-86-158, MRC-R-976, Mission Research Corporation, May 1986.

3. Dana, R. A., *ACIRF User's Guide. Volume I: Theory and Examples*, MRC-R-1198, Mission Research Corporation, December 1988.

4. Knepp, D. L., "Aperture Antenna Effects After Propagation Through Strongly Disturbed Random Media," *IEEE Transactions on Antennas and Propagation*, Vol. AP-33, No. 10, pp. 1074-84, October 1985.

DISTRIBUTION LIST

DNA-TR-89-262

DEPARTMENT OF DEFENSE

ASSISTANT TO THE SECRETARY OF DEFENSE
ATTN: EXECUTIVE ASSISTANT

DEFENSE ADVANCED RSCH PROJ AGENCY
ATTN: CHIEF SCIENTIST
ATTN: GSD R ALEWINE

DEFENSE COMMUNICATIONS AGENCY
ATTN: DR P CROWLEY
ATTN: J DIETZ
ATTN: SSS

DEFENSE COMMUNICATIONS ENGINEER CENTER
ATTN: CODE R410

DEFENSE INTELLIGENCE AGENCY
ATTN: DB-TPO
ATTN: DC-6
ATTN: DIR
ATTN: DT-1B
ATTN: RTS-2B

DEFENSE NUCLEAR AGENCY
ATTN: DFSP G ULLRICH
ATTN: DFSP G ULLRICH
ATTN: NANF
ATTN: NASF
ATTN: OPNA
ATTN: PRPD R YOHO
3 CYS ATTN: RAAE
ATTN: RAAE A CHESLEY
ATTN: RAAE A MARDIGUIAN
ATTN: RAAE D RIGGIN
ATTN: RAAE G ULLRICH
ATTN: RAAE K SCHWARTZ
ATTN: RAAE M CRAWFORD
ATTN: RAAE S BERGGREN
ATTN: RAEE
4 CYS ATTN: TITL

DEFENSE NUCLEAR AGENCY
ATTN: TDNM
2 CYS ATTN: TDTT W SUMMA

DEFENSE TECHNICAL INFORMATION CENTER
2 CYS ATTN: DTIC/FDAB

JOINT DATA SYSTEM SUPPORT CTR
ATTN: JNSV

NATIONAL SECURITY AGENCY
ATTN: L PLUSWICK

STRATEGIC AND THEATER NUCLEAR FORCES
ATTN: DR E SEVIN
ATTN: DR SCHNEITER
ATTN: LC R DAWSON

STRATEGIC DEFENSE INITIATIVE ORGANIZATION
ATTN: EN
ATTN: EN LTC C JOHNSON
ATTN: PTP LTC SEIBERLING
ATTN: TN

STRATEGIC TARGET PLANNING
ATTN: JKC (ATTN: DNA REP)
ATTN: JKCS
ATTN: JLWT (THREAT ANALYSIS)
ATTN: JPEM
ATTN: JPSS

THE JOINT STAFF
ATTN: J6

U S NUCLEAR CMD & CENTRAL SYS SUPPORT STAFF
ATTN: SAB H SEQUINE

DEPARTMENT OF THE ARMY

ARMY LOGISTICS MANAGEMENT CTR
ATTN: DLSIE

HARRY DIAMOND LABORATORIES
ATTN: SLCIS-IM-TL (TECH LIB)

INFORMATION SYSTEMS COMMAND
ATTN: STEWS-TE-N K CUMMINGS

U S ARMY ATMOSPHERIC SCIENCES LAB
ATTN: SLCAS-AE (DR NILES)
ATTN: SLCAS-AE-E
ATTN: SLCAS-AR DR H HOLT

U S ARMY COMMUNICATIONS R&D COMMAND
ATTN: AMSEL-RD-ESA

U S ARMY FOREIGN SCIENCE & TECH CTR
ATTN: DRXST-SD

U S ARMY MISSILE COMMAND
ATTN: AIAMS-S/B J GAMBLE

U S ARMY MISSILE COMMAND/AMSMI-RD-CS-R
ATTN: AMSMI-RD-CS-R (DOCS)

U S ARMY NUCLEAR & CHEMICAL AGENCY
ATTN: MONA-NU

U S ARMY NUCLEAR EFFECTS LABORATORY
ATTN: ATAA-PL
ATTN: ATAA-TDC
ATTN: ATRC-WCC LUIS DOMINCUEZ

U S ARMY STRATEGIC DEFENSE CMD
ATTN: CSSD-H-LS B CARRUTH
ATTN: CSSD-H-SA
ATTN: CSSD-H-SAV
ATTN: CSSD-IN-T M POPE
ATTN: CSSD-SA-EV RON SMITH

U S ARMY STRATEGIC DEFENSE COMMAND
ATTN: ATC-O W DAVIES
ATTN: CSSD-GR-S W DICKINSON

USA SURVIVABILITY MANAGMENT OFFICE
ATTN: SLCSM-SE J BRAND

DEPARTMENT OF THE NAVY

COMMAND & CONTROL PROGRAMS
ATTN: OP 941

DEPARTMENT OF THE NAVY
ATTN: JCMG-707

NAVAL AIR SYSTEMS COMMAND
ATTN: PMA 271

NAVAL ELECTRONICS ENGRG ACTVY, PACIFIC
ATTN: CODE 250

NAVAL OCEAN SYSTEMS CENTER
ATTN: CODE 542, J FERGUSON

NAVAL RESEARCH LABORATORY
ATTN: CODE 2000 J BROWN
ATTN: CODE 2627 (TECH LIB)
2 CYS ATTN: CODE 4100 H GURSKY
ATTN: CODE 4121.8 H HECKATHORN
ATTN: CODE 4183
ATTN: CODE 4700 S OSSAKOW
ATTN: CODE 4701
ATTN: CODE 4720 J DAVIS
ATTN: CODE 4780 B RIPIN
ATTN: CODE 4780 DR P BERNHARDT
ATTN: CODE 4780 J HUBA
ATTN: CODE 4785 P RODRIGUEZ
ATTN: CODE 5300
ATTN: CODE 5326 G A ANDREWS
ATTN: CODE 5340 E MOKOLE
ATTN: CODE 8344 M KAPLAN

NAVAL SURFACE WARFARE CENTER
ATTN: CODE H-21

NAVAL TECHNICAL INTELLIGENCE CTR
ATTN: DA44

NAVAL UNDERWATER SYSTEMS CENTER
ATTN: CODE 3411, J KATAN

OFFICE OF CHIEF OF NAVAL OPERATIONS
ATTN: OP 654
ATTN: OP 941D
ATTN: OP 981N

OFFICE OF NAVAL RESEARCH
ATTN: A TUCKER

SPACE & NAVAL WARFARE SYSTEMS CMD
ATTN: CODE 3101 T HUGHES
ATTN: PD 50TD
ATTN: PD50TD1 G BRUNHART
ATTN: PME 106-4 S KEARNEY
ATTN: PME-106 F W DIEDERICH

THEATER NUCLEAR WARFARE PROGRAM OFC
ATTN: PMS-42331F (D SMITH)

DEPARTMENT OF THE AIR FORCE

AFIA/INIS
ATTN: AFIA/INKD MAJ SCHROCK

AIR FORCE CTR FOR STUDIES & ANALYSIS
ATTN: AFCSA/SAMI
ATTN: AFCSA/SASC

AIR FORCE ELECTRONIC WARFARE CENTER
ATTN: LT M MCNEELY

AIR FORCE GEOPHYSICS LABORATORY
ATTN: J KLOUBACHAR
ATTN: OP/W BLUMBERG
ATTN: SANTI BASU

AIR FORCE OFFICE OF SCIENTIFIC RSCH
ATTN: AFOSR/NP

AIR FORCE SYSTEMS COMMAND
ATTN: XTWT, MAJOR W G CLARK

AIR FORCE TECHNICAL APPLICATIONS CTR
ATTN: TN

AIR UNIVERSITY LIBRARY
ATTN: AUL-LSE

HQ AWS, DET 3 (CSTC/WE)
ATTN: WE

NATIONAL TEST FACILITY
ATTN: NTB/JPO DR C GIESE

STRATEGIC AIR COMMAND/XRFS
ATTN: XRFS

WEAPONS LABORATORY
ATTN: NTCA
ATTN: NTN
ATTN: WL/SUL

DEPARTMENT OF ENERGY

EG&G, INC
ATTN: D WRIGHT

LAWRENCE LIVERMORE NATIONAL LAB
ATTN: T DONICH

LOS ALAMOS NATIONAL LABORATORY
ATTN: R W WHITAKER/ESS-5

SANDIA NATIONAL LABORATORIES
ATTN: P L MATTERN

SANDIA NATIONAL LABORATORIES
ATTN: A D THORNBROUGH
ATTN: R BACKSTROM
ATTN: D DAHLGREN
ATTN: ROBERT M AXLINE
ATTN: ORG 1231, J R LEE
ATTN: ORG 9114 W D BROWN
ATTN: TECH LIB

OTHER GOVERNMENT

CENTRAL INTELLIGENCE AGENCY
ATTN: OSWR/NED
ATTN: OSWR/SSD FOR L BERG

DEPARTMENT OF COMMERCE
ATTN: G REEVE
ATTN: J HOFFMEYER
ATTN: W UTLAUT

DEPARTMENT OF DEFENSE CONTRACTORS

AEROSPACE CORP
ATTN: A MORSE
ATTN: BRIAN PURCELL
ATTN: C CREWS
ATTN: C RICE
ATTN: DR J M STRAUS
ATTN: G LIGHT
ATTN: I GARFUNKEL
ATTN: J KLUCK
ATTN: M ROLENZ

ANALYTICAL SYSTEMS ENGINEERING CORP
ATTN: SECURITY

AT&T BELL LABORATORIES
ATTN: DENIS S LONGO
ATTN: JOSEPH A SCHOLL

ATLANTIC RESEARCH SERVICES CORP
ATTN: R MCMILLAN

ATMOSPHERIC AND ENVIRONMENTAL RESEARCH INC
ATTN: M KO

AUSTIN RESEARCH ASSOCIATES
ATTN: J THOMPSON

AUTOMETRIC INCORPORATED
ATTN: C LUCAS

BDM INTERNATIONAL INC
ATTN: W LARRY JOHNSON

BDM INTERNATIONAL INC
ATTN: L JACOBS

BERKELEY RSCH ASSOCIATES, INC
ATTN: C PRETTIE
ATTN: J WORKMAN
ATTN: N T GLADD
ATTN: S BRECHT

BOEING CO
ATTN: G HALL

CALIFORNIA RESEARCH & TECHNOLOGY, INC
ATTN: M ROSENBLATT

CHARLES STARK DRAPER LAB, INC
ATTN: A TETEWSKI

COMMUNICATIONS SATELLITE CORP
ATTN: RICHARD A ARNDT

CORNELL UNIVERSITY
ATTN: D FARLEY JR
ATTN: M KELLY

DEFENSE GROUP, INC
ATTN: M K GROVER

ELECTROSPACE SYSTEMS, INC
ATTN: LINDA CALDWELL/LIBRARIAN
ATTN: P PHILLIPS

EOS TECHNOLOGIES, INC
ATTN: B GABBARD
ATTN: R LELEVIER

GENERAL ELECTRIC CO
ATTN: ROBERT H EDSALL

GENERAL RESEARCH CORP INC
ATTN: J EOLL

GEO CENTERS, INC
ATTN: E MARRAM

GRUMMAN AEROSPACE CORP
ATTN: J DIGLIO

HARRIS CORPORATION
ATTN: E KNICK

HSS, INC
ATTN: D HANSEN

INFORMATION SCIENCE, INC
ATTN: W DUDZIAK

INSTITUTE FOR DEFENSE ANALYSES
ATTN: E BAUER
ATTN: H WOLFHARD

J S LEE ASSOCIATES INC
ATTN: DR J LEE

JAYCOR
ATTN: J SPERLING

JOHNS HOPKINS UNIVERSITY
ATTN: C MENG
ATTN: H G TORNATORE
ATTN: J D PHILLIPS
ATTN: R STOKES

KAMAN SCIENCES CORP
ATTN: DASIAC
ATTN: E CONRAD
ATTN: G DITTBERNER

KAMAN SCIENCES CORPORATION
ATTN: B GAMBILL
ATTN: DASIAC
ATTN: R RUTHERFORD

LOCKHEED MISSILES & SPACE CO, INC
ATTN: J HENLEY
ATTN: J KUMER
ATTN: R SEARS

LOCKHEED MISSILES & SPACE CO, INC
ATTN: D KREJCI
ATTN: D T RAMPTON

LTV AEROSPACE & DEFENSE COMPANY
2 CYS ATTN: LIBRARY EM-08

M I T LINCOLN LAB
ATTN: D TOWLE
ATTN: I KUPIEC

MARTIN MARIETTA DENVER AEROSPACE
ATTN: J BENNETT
ATTN: H VON STRUVE III

MAXIM TECHNOLOGIES, INC
ATTN: B RIDGEWAY
ATTN: J SCHLOBOHM

MCDONNELL DOUGLAS CORP
ATTN: T CRANOR

MCDONNELL DOUGLAS CORPORATION
ATTN: J GROSSMAN
ATTN: R HALPRIN

METATECH CORPORATION
ATTN: R SCHAEFER
ATTN: W RADASKY

METEOR COMMUNICATIONS CORP
ATTN: R LEADER

MISSION RESEARCH CORP
ATTN: J KENNEALY
ATTN: R ARMSTRONG
ATTN: S DOWNER
ATTN: W WHITE

MISSION RESEARCH CORP
ATTN: R L BOGUSCH

MISSION RESEARCH CORP
ATTN: DAVE GUICE

MISSION RESEARCH CORP
ATTN: B R MILNER
ATTN: C LONGMIRE
ATTN: D ARCHER
ATTN: D KNEPP
ATTN: D LANDMAN
ATTN: F FAJEN
ATTN: F GUIGLIANO
ATTN: G MCCARTOR
ATTN: K COSNER
ATTN: M FIRESTONE
ATTN: R BIGONI
ATTN: R DANA
ATTN: R HENDRICK
ATTN: R KILB
ATTN: S GUTSCHE
2 CYS ATTN: S M FRASIER
ATTN: TECH LIBRARY

MITRE CORPORATION
ATTN: DR M R DRESP

MITRE CORPORATION
ATTN: M HORROCKS
ATTN: R C PESCI
ATTN: W FOSTER

NORTHWEST RESEARCH ASSOC, INC
ATTN: E FREMOUW

PACIFIC-SIERRA RESEARCH CORP
ATTN: E FIELD JR
ATTN: F THOMAS
ATTN: H BRODE

PHOTOMETRICS, INC
ATTN: I L KOFSKY

PHOTON RESEARCH ASSOCIATES
ATTN: D BURWELL
ATTN: O LEWIS

PHYSICAL RESEARCH INC
ATTN: W SHIH

PHYSICAL RESEARCH INC
ATTN: A CECERE

PHYSICAL RESEARCH INC
ATTN: H FITZ
ATTN: P LUNN

PHYSICAL RESEARCH, INC
ATTN: R DELIBERIS
ATTN: T STEPHENS

PHYSICAL RESEARCH, INC
ATTN: J DEVORE
ATTN: J THOMPSON
ATTN: W SCHLUETER

PHYSICS INTERNATIONAL CO
ATTN: C GILMAN

R & D ASSOCIATES
ATTN: C GREIFINGER
ATTN: F GILMORE
ATTN: G HOYT
ATTN: L DERAAD

R & D ASSOCIATES
ATTN: J WALTON

RAND CORP
ATTN: C CRAIN
ATTN: E BEDROSIAN

RAND CORP
ATTN: B BENNETT

RJO ENTERPRISES/POET FAC
ATTN: STEVEN KRAMER
ATTN: W BURNS

S-CUBED
ATTN: C NEEDHAM
ATTN: T CARNEY

SCIENCE APPLICATIONS INTL CORP
ATTN: C SMITH
ATTN: D HAMLIN
ATTN: D SACHS
ATTN: L LINSON

SCIENCE APPLICATIONS INTL CORP
ATTN: J COCKAYNE

SCIENCE APPLICATIONS INTL CORP
ATTN: H SUNKENBERG
ATTN: LIBRARY

SCIENCE APPLICATIONS INTL CORP
ATTN: S ROSENCWEIG

SRI INTERNATIONAL
ATTN: R LIVINGSTON
ATTN: R T TSUNODA
ATTN: W CHESNUT
ATTN: W JAYE

STEWART RADIANCE LABORATORY
ATTN: R HUPPI

TELECOMMUNICATION SCIENCE ASSOCIATES
ATTN: R BUCKNER

TELEDYNE BROWN ENGINEERING
ATTN: J WOLFSBERGER, JR
ATTN: N PASSINO

TOYON RESEARCH CORP
ATTN: J ISE

TRW INC
ATTN: DR D GRYBOS
ATTN: ED SIMMONS

TRW SPACE & DEFENSE SECTOR SPACE &
ATTN: D M LAYTON

USER SYSTEMS, INC
ATTN: S W MCCANDLESS, JR

UTAH STATE UNIVERSITY
ATTN: K BAKER
ATTN: L JENSEN

VISIDYNE, INC
ATTN: J CARPENTER

DIRECTORY OF OTHER

BOSTON UNIVERSITY
ATTN: MICHAEL MENDILLO